STRUCTURAL FIRE PERFORMANCE OF FIBER-REINFORCED HSC BEAMS USING OPENSEES SOFTWARE

By

Shahzada Khuram

(NUST201362914MSCEE15213F)

Master of Science

in

Structural Engineering

NUST Institute of Civil Engineering (NICE)

School of Civil and Environmental Engineering (SCEE)

National University of Sciences and Technology (NUST)

Islamabad, Pakistan

2017

This is to certify that the

thesis titled

STRUCTURAL FIRE PERFORMANCE OF FIBER-REINFORCED HSC BEAMS USING OPENSEES SOFTWARE

submitted by

Shahzada Khuram

(NUST201362914MSCEE15213F)

has been accepted towards the partial fulfillment

of the requirements for the degree

of

Master of Science

in

Structural Engineering

Dr. Syed Hassan Farooq (Advisor)
Assistant Professor
NUST Institute of Civil Engineering (NICE)
School of Civil and Environmental Engineering (SCEE)
National University of Sciences and Technology (NUST), Islamabad, Pakistan

THESIS ACCEPTANCE CERTIFICATE

Certified that final copy of MS thesis written by Mr Shahzada Khuram, Registration No. NUST201362914MSCEE15213F, of MS Structure 2013 Batch (NICE) has been vetted by undersigned, found completed in all respects as per NUST Statutes/Regulations, is free of plagiarism, errors, and mistakes and is accepted as partial fulfilment for award of MS degree. It is further certified that necessary amendments as pointed out by GEC members of the scholar have been incorporated in the said thesis.

Signature_____

Name of Supervisor: Dr Syed Hassan Farooq

Date: _____

Signature (HoD)_____

Date: _____

Signature (Dean/Principal)_____

Date:_____

DEDICATED

TO

MY BELOVED PARENTS AND FAMILY

ACKNOWLEDGEMENTS

I wish to express my greatest gratitude to my research advisors Dr Syed Hassan Farooq and Dr Wasim Khaliq, Faculty of Structural Department (NICE-NUST) for their continuous, unconditional support and guidance all over this work. I am deeply thankful to them for their motivation all along this journey. Special thanks for their countless hours of reflecting, reading, encouraging and greatest of all patience throughout the entire process.

I would like to pay special thanks to my distinguished faculty members. I pay my special gratitude to Dr Syed Ali Rizwan and Dr Rao Arsalaan Khushnood who were there to help me all the time.

I am also very grateful to my brother Dr Muhammad Arshad, Associate Professor, Institute of Environmental Sciences and Engineering (IESE) for his continuous support during course of this study. Special thanks to my colleagues especially to Mr Saif Ur Rehman and Mr Shahzada Khuram for their countless help and cooperation during this thesis work. I would like to pay my regards to staff of NICE for their assistance and help during course work and analytical study.

At last I would also like to appreciate the support and efforts of my wife who has been taking care of all my administrative requirements and taking care of my home.

ABSTRACT

Fire resistance is one of the significant properties of the normal-strength concrete, however, the new types of concretes such as fiber-reinforced concrete (FRC), high-strength concrete (HSC), Self-consolidating concrete (SCC), and Fly-ash concrete (FAC) may not show the same level of resistance to fire. It is because of the quicker dilapidation of strength at higher temperatures and the occurrence of fire-induced spalling.

Structures modelling using computers subjected to extreme dynamic and static loads (such as wind, snow, earthquake, and impact) using finite-element software are very common and extensively being used in construction industry. However, to study the structure response of fire, highly tedious nature of modelling the full (often coupled) sequence of a realistic fire scenario, heat transfer to structure and structural response is required and only a few of the top consulting engineers in the world truly specialize in this niche area (Jiang et al. 2013).

Tests to judge and quantify the structural fire performance of High Performance Concrete (HSC) are very expensive, time consuming and limited in varying parameters. Computer simulations/modelling is an alternative which is practicable, reliable and has versatility in varying parameters. There are currently very limited data on the high-temperature tensile strength properties of HSC, fiber-reinforced HSC (FRHSC), SCC, and FAC. There is a need to simulate the high-temperature tensile strength properties of HSC, FRHSC, SCC, and FAC.

An object-oriented software framework, known as OpenSees which is the acronym of Open System for Earthquake Engineering Simulation created at the National Science Foundation. It facilitates users to generate finite element applications for simulating the structural and geotechnical response systems subjected to earthquakes (Usmani et al. 2012). The OpenSees Developers Group at the University of Edinburgh has included thermal capabilities in OpenSees. The advantage to extend existing finite-element codes is due to its ability to perform multihazard

type analysis as opposed to creating fire-specific applications, e.g., fire succeeding to earthquake. The OpenSees software is open source and object oriented framework that's why it is used for this purpose. The OpenSees framework was initially designed for the earthquake analysis of structures and is extended by the addition of new concrete classes for temperature distributions across element cross sections, thermal loads, and material laws based on Eurocodes (Jiang et al. 2013). This study is carried out to enable thermomechanical analysis of High Performance Reinforced beams with and without fibers) using software framework of OpenSees.

TABLE OF CONTENTS

LIST OF FIGURES

LIST OF TABLES

CHAPTER 1

INTRODUCTION

1.1 General

A most commonly used construction material is Concrete due to versatility in its application (Dwaikat 2009) and excellent strength, durability, ease of fabrication, and fire resistance properties (Khaliq and Kodur 2013). When concrete constituents (i.e. aggregates and cement) combined chemically, form an essentially inert material having a poor thermal conductivity and low strength loss properties. Generally, it provides excellent fire resistance properties, non-combustible and when exposed to fire, toxic fumes, smoke etc does not emit thus finds major applications in built infrastructures specially buildings, where one of the primary considerations is fire safety. In constructions like high rise buildings infrastructures and primarily in nuclear power plants high strength concrete is extensively being used. In some of HSC structures exposed to severe fire conditions have performed poorly. In recent years, the HSC was mainly used in bridges, infrastructure projects and off-shore structures, and has been extended to columns and beams in reinforced concrete (RC) buildings. Fire is one of the severe hazard to which structures may be exposed during their entire life and hence the provision of appropriate fire resistance measures is an important aspect of building design. This is to enhance safety of occupants, control the spread of fire, and minimize damage to property and environment in the event of a fire in the building. Fire safety design can be achieved through active and passive fire protection measures. Active systems generally get self-activated once the fire is triggered and they include fire detectors, smoke control systems, and sprinklers. Passive systems are built into the structure (buildings), and do not require specific operation to control the fire. The need for passive fire protection systems or what is commonly referred to as fire resistance, can be due to the fact that structural integrity is the last safety factor when other factors for containing the fire flop. Definition of fire resistance is the duration during

which a structural member (system) shows resistance with referenece to stability, structural integrity, and temperature transmission when exposed to fire (Buchanan 2002). Conventional normal strength concrete (NSC) members generally exhibit good fire resistance. However, some studies show that structural members made of new concrete types (HSC, SCC and FAC) have lower fire resistance properties (Bamonte et al. 2010; Kodur ; Tang and Lo 2009). This has been due to differences in thermo-mechanical properties of HSC, SCC and FAC and also to the occurrence of fire induced spalling (Castillo and Durrani 1990); (Kodur and Sultan 1998; Tang and Lo 2009). It has also been shown that the spalling in HSC members can be overcome through the addition of fibers (steel, propylene, and hybrid) in the concrete mix. Whilst most of the high temperature properties are available for NSC, no data is available for new types of HSC such as SCC, and FAC (plain and with different fiber combinations).

1.2 Concrete properties at high temperature

Constituent materials properties at elevated temperature are required to evaluate fire resistance of a structural system (Buchanan 2002). For analysis of fire resistance, thermal, mechanical, deformation properties of concrete are needed and special properties such as fire induced spalling is also required. Thermal conductivity, thermal expansion, specific heat, thermal diffusivity, and mass loss are included in thermal properties. Creep and mechanical properties like strength, stress-strain curves, and elastic modulus considerably influence the fire response of a structural system. Spalling induced by fire occurs in concrete under certain fire conditions can also alter the response of a RC structural system. These properties vary with change in temperature and are influenced by the type of aggregate, mix proportions, mineral and chemical admixtures, and presence of fibers(Bazant and Kaplan 1996; Buchanan 2002; DiNenno 2008; Phan 1996). HSC are typically made through addition of binders such as silica fume, fly ash, blast furnace slag, and other smaller amounts of mineral and chemical admixtures. These binders introduce specific properties to HSC such as flow ability and workability in fresh form

and high strength and dense microstructure in the hardened form. Thus thermal and mechanical properties of HSC can be different from that of conventional concrete (Kodur and Sultan 1998). When these HSC's are subjected to high temperatures, their performance is affected by changes in its thermal and mechanical behavior. Understanding the behavior of these HSC's at the material level and characterizing their high temperature properties is important for predicting the fire response of HSC structural members. However, at present there is very limited information on high temperature thermal and mechanical properties for these new types of HSC.

1.3 HSC beam response under fire

The fire response of HSC beams is influenced by the properties of concrete and reinforcing steel. These include thermal, mechanical and deformation properties at room as well at high temperatures. The thermal properties govern the extent of heat transfer, while mechanical properties (strength and stiffness) determine the load carrying capacity and deformation of the structural member. The deformation properties such as creep and thermal expansion determine the extent of deformation in the member.

1.4 Need of computational modelling

Tests to judge and quantify the structural fire performance of High Strength Concrete (HSC) are very expensive, time consuming and limited in varying parameters. Computer simulations / modelling is an alternative which is practicable, reliable and has versatility in varying parameters. There are currently very limited data on the high-temperature tensile strength properties of HSC, fiber-reinforced HSC (FRHSC), SCC, and FAC. There is a need to simulate the high-temperature tensile strength properties of HSC, FRHSC, SCC, and FAC.

1.5 Research objectives

The difference in fire behaviour of NSC and HSC beams results from different mechanical and thermal properties at elevated temperature. With the increased use of new types of HSC in RC beams, there is a need to characterize its thermal and mechanical properties both at material and structural level.

From the above discussion, it is evident that one of the important point for using HSC in beams is the deficiency of knowledge about the structural response of HSC-strengthened systems under fire. This study examines the implications of high temperature thermal susceptibility on currently used materials in civil engineering applications and on structural behavior of HSC-strengthened RC beams using OpenSees Software. To achieve this objective, extensive literature review followed by development of computer model and parametric studies on HSC-strengthened RC beams have been conducted. Specific objectives of this research are:

- Learn OpenSees Software with a focus on its extension for analysis of concrete members in fire.
- Include HSC into existing material library of OpenSees
- Conduct fire analysis of Reinforce Concrete using newly incorporated material.
- Develop and validate a general, flexible and extensible thermal analysis of HSC for "structures in fire" using OpenSees.

1.6 Scope and outline

The work presented in this thesis involves development and application of a numerical model. The numerical work involved development of a new material HSC in OpenSees and its application in RC beams. The model was validated by using the test data generated from current fire tests and data available in the literature. The validated model was then applied to undertake

parametric studies to compute influence of various factors on fire response of HSC-strengthened RC beams. The thesis is organized into five chapters:

- Chapter 1 provides background information on fire resistance of HSC and elevated temperature properties needed for fire resistance evaluation of HSC beams using OpenSees.
- Chapter 2 provides a review of the literature on the high temperature thermal and mechanical material properties of conventional NSC and HSC, the variability in existing data and also highlights limitations of available methods for fire resistance evaluation of HSC beams.
- Chapter 3 presents the introduction of HSC into OpenSees material library and its validation.
- In Chapter 4 analytical studies on high temperature mechanical properties of HSC are presented. The results obtained from the OpenSees are also discussed with the possible logics and reasoning.
- Chapter 5 abridges the key findings, narrates conclusions and suggests recommendations based on the study.

CHAPTER 2

STATE-OF-THE-ART REVIEW

2.1 General

Generally concrete has good fire resistance properties and thus used extensivelly in buildings and other built infrastructure, where fire safety is an important concern. However, recently it is observed that structural members made of new concrete types like HSC, may not have same level of fire resistance like conventional concrete (NSC) (Bamonte et al. 2010; Kodur and Ahmed 2010; Tang and Lo 2009). Typically, new types of HSC have lots of applications in beams of building because of the advantage of higher strength which is utilized to reduce size (cross-section) of beams. The fire resistance of concrete structural members is governed by high temperature thermal and mechanical properties of constituent concrete. For predicting fire resistance of concrete structural members, knowledge of high temperature material properties is very critical which includes thermal, mechanical and deformation properties. In addition to that, fire induced spalling might expressively influence resistance of HSC in the fire, therefore properties related to spalling are also important and should be known.

In this chapter, previous studies related to the elevated temperature properties of concrete and reinforcing steel are reviewed.

2.2 Concrete

2.2.1 General

Concrete is a non-combustible construction material that do not contribute readily to heat transfer (good insulating material) (Kodur and Ahmed 2010). Concrete undergoes physiochemical changes when heated and the influence of temperature is different for sealed and unsealed concrete. Strength loss in concrete depends on cement blend used in the mix and type of aggregate and is negligible up to 300°C. However, this temperature range of mechanical

properties deterioration can be enhanced to 500°C by careful concrete mix design (Khoury 2000). Creep strains in concrete gets significant at about 550-600°C, thus, deformations in concrete can be significant above 600°C.

2.2.2 Thermal properties

2.2.2.1 General

Specific heat (heat capacity) and thermal conductivity are the two properties that influence thermal response of HSC RC beams. In literature, there is available test data on characterizing thermal properties of concrete at high temperatures (Kodur and Sultan 2003; Lie and Kodur 1996; Lie and Kodur 1995) ;(Saad et al. 1996) ;(Shin et al. 2002) ;(Van Geem et al. 1997). These properties significantly depend on type of aggregate (siliceous, carbonate or light weight) used in the concrete.

Figure 2.1 and Figure 2.2 shows the change in specific heat and thermal conductivity of normal strength concrete (NSC) as a function of temperature as given in ASCE Manual (1992) and Eurocode 2 (2004) and upper and lower range of values from published test data (shown in solid lines). There is considerable discrepancy in test data which can be attributed to differences in test procedure and measuring techniques. Type of aggregate has considerable influence on thermal properties of concrete. Peaks observed in heat capacity of carbonate aggregate, in the temperature range of 600-800°C is caused by the endothermic reaction because of decomposition of dolomite. This reaction consumes large amount of heat energy and this helps to enhance fire resistance.

The elastic modulus variation with temperature for different concrete types is shown in Figure 2.3 Elastic modulus changes of concrete as function of temperature). In general, the modulus of elasticity if concrete decreases significantly with increase in temperature. Studies have shown that type of aggregate in concrete slightly effect the rate of decrease of elastic modulus.

In the tests conducted by (Schneider 1988), the author reports that factors such as original strength and water-cement ratio do not significantly affect the elastic modulus at elevated temperatures.

Figure 2.5 and Figure 2.6 show the variation of compressive strength with temperature for normal and high strength concretes, respectively. For normal strength concrete (NSC), there is not much variation in compiled test data. The data for high strength concrete (HSC) shows a large variation especially in the range of 200-500°C. This variation can be attributed to various factors such as occurrence of concrete spalling during testing, variation in testing procedure (different heating and loading rate), test conditions, limitations of testing apparatus, and measuring techniques. This test data formed the basis of constitutive relationships for high temperature mechanical properties of concrete. These relationships are presented in ASCE Manual, Eurocode 2 and (Kodur et al. 2004).

The residual strength of concrete is an important property for modelling structural members exposed to design fire. During cooling phase under design fire, the process of hydration of unhydrated cement components is an ongoing process. These hydrated products have larger volume that introduces cracking in concrete, thus, concrete continues to lose strength and stiffness (Dwaikat 2009). Thus, the residual strength of concrete is less than heated concrete. Data published in literature shows that there is a large variation in residual strength of concrete, as shown in Figure 2.4. This large variation can be attributed to using different heating (or cooling) or loading rate, specimen and test conditions, and the use of admixtures.

Codes and standards, such as Eurocode 2 and ASCE manual, do not specify relationships for the residual strength of concrete after fire exposure. However, best fit of the published test data is generally used for evaluating the residual strength of concrete, as shown in Figure 2.4 (Kumar and Kumar 2003).

For evaluating fire resistance of concrete structural members the temperature distribution within the member is to be established. This temperature distribution is dependent on high temperature thermal properties of concrete. The thermal properties that govern the temperature distribution are thermal conductivity and specific heat (or heat capacity).

Other thermal properties that influence the fire behavior of RC structural members are thermal expansion and mass loss that influence development of thermal stresses and specific heat respectively. Thermal conductivity is "the rate of heat flow ratio to temperature gradient, and shows the unvarying heat flow through unit thickness of concrete over a unit area exposed to a unit temperature difference between the opposite two faces". Concrete holds moisture in different arrangements and quantity of it has substantial effect on thermal conductivity. Thermal conductivity is generally computed by using 'steady state' or 'transient' test methods (Bazant and Kaplan 1996). For moist concrete transient methods are favoured over steady-state methods to measure thermal conductivity (Shin et al. 2002), as physicochemical variations of concrete at elevated temperatures cause irregular direction of heat flow. The amount of heat per unit mass is specific heat, required to vary the temperature of a material by one degree and is generally stated in terms of thermal (heat) capacity which is the product of density and specific heat. Specific heat is highly influenced by aggregate type, density, and moisture content of concrete (Kodur and Sultan 1998; Phan and Carino 1998).

Specific heat represents the energy absorbed by the concrete and accounts for sensible heat and latent heat involved during temperature change. Sensible heat ascribes to the heat involved in thermodynamic reaction during temperature change. Latent heat refers to the energy absorbed or released by the material during phase transition. The material absorbs considerable amount of energy during physiochemical changes and hence specific heat values are highly influenced by the phase transition in materials.

The percentage change in length of a specimen per degree temperature increase is the coefficient of thermal expansion. Linear thermal expansion is the thermal strain causing due to increased temperature. Thermal expansion of concrete is generally depend upon cement type, aggregate type, water content, age and temperature (Lie 1992). Concrete thermal expansion gets complex by factors like additional volume changes caused by variations in moisture content, by chemical reactions (composition change, dehydration), and by micro-cracks and creep resulting from non-uniform thermal stresses (Bazant and Kaplan 1996). In some cases, loss of water occurs due to heating which causes thermal shrinkage along with thermal expansion, and overall might lead to to be negative volume change, i.e. shrinkage rather than expansion.

2.2.2.2 Previous studies on thermal properties

There have been quite a few test programs for characterizing high temperature thermal properties of concrete(Harmathy and Allen 1973; Lie and Kodur 1996; Van Geem et al. 1997) (Shin et al. 2002) and (Kodur and Sultan 2003)have evaluated the thermal properties 21 of NSC concrete. Based on the test data, empirical formulae for thermal properties of NSC have been developed (ASCE, 1992; Eurocode 2, 2004). Some of the notable studies are reviewed here:

(Harmathy and Allen 1973) studied the effect of temperature on thermal properties of NSC through thermogravimetry and dilatometry tests. In these tests the temperature of the specimen was raised form room temperature to 1000°C at a rate of 5°C/min and thermal properties namely, thermal conductivity, specific heat, thermal diffusivity, and mass loss were measured. It was concluded by the authors that heat flow in concrete at elevated temperatures cannot be accurately predicted unless latent heat effects associated with the process are properly considered. It was found that variation in apparent specific heat due to elevated temperatures

was difficult to obtain and supplemental theoretical considerations were suggested. It was also concluded that the spalling of concrete in fire is not caused by the presence of quartz in the aggregate, but it is due to high moisture content in concrete.

(Lie and Kodur 1996) measured high temperature thermal properties of steel fiber reinforced concrete in 0-1000°C range. These thermal properties comprised of specific heat, thermal conductivity, mass loss, and thermal expansion. They also proposed empirical relations for these properties as a function of temperature. It was concluded by the authors that thermal properties of steel fiber reinforced concrete are like conventional plain NSC. They proposed mathematical relations that can be used as input data in analytical models for fire resistance calculations of structural members.

(Van Geem et al. 1997) experimentally investigated thermal properties of HSC at elevated temperatures. The HSC used in this study ranged from 69-138 MPa with water to cement ratio ranging from 0.26 to 0.32. Mineral admixtures such as silica fume and fly ash were also used in 22 the concrete mixes. They tested thermal conductivity, specific heat, thermal diffusivity and drying rates at 30, 150, and 370°C. They used different test methods to evaluate the thermal properties and found that these properties differed depending upon the test method used. Thermal conductivity using hot plate method, hot wire method and graduated hot plate apparatus was found to be similar and was within 1.7 to 2.6 W/m.K range. It was found that thermal conductivity of HSC decreases with increasing temperature. The specific heat values of HSC were also reported to be similar to those conventional NSC. Thermal diffusivity of HSC reduced with increasing temperature and was found to decrease significantly at 540°C and was attributed to increase rate of mass loss near this temperature. Mass loss of HSC was also found to be similar to that of NSC at elevated temperatures.

(Shin et al. 2002) experimentally studied the thermal behavior of indigenous Korean concrete mixes (similar to US basaltic concrete) exposed to high temperature conditions. They tested

density, thermal conductivity, thermal diffusivity and specific heat in 20-1100°C temperature range. It was found that most thermal properties except for specific heat decrease with increasing temperature. The thermal properties of concrete were found to be strongly temperature dependent. The density, thermal conductivity, and thermal diffusivity decrease with temperature, and particularly the conductivity and the diffusivity which have a 50% decrease at 900°C as compared to room temperature values. The specific heat was found to increase until 500°C, decrease in 700 to 900°C temperature range, and then increase again above 900°C. It was also concluded that the measurement beyond 1100°C is not accurate enough because the concrete decomposes to a liquid phase from a solid phase at that temperature.

(Kodur and Sultan 2003) also carried out tests to measure thermal conductivity, specific heat, thermal expansion, and mass loss of plain HSC and steel fiber-reinforced HSC made of siliceous 23 and carbonate aggregate. Based on the measured property data, empirical relations were proposed for thermal properties as a function of temperature in the temperature range of 0 and 1000°C. It was concluded in this study that the type of aggregate has a significant influence on the thermal properties of HSC at elevated temperatures. The measured results showed that the presence of carbonate aggregate in HSC increases fire resistance. The authors also concluded that the thermal properties, at elevated temperatures, exhibited by steel fiber-reinforced HSC are similar to those of plain HSC.

Hu et al. (1993) investigated the thermal properties of construction materials commonly available in China. In this study mass loss was measured as a function of temperature up to 1000°C. It was found in this study that mass loss in carbonate aggregate concrete was only up to 97% for temperature up to 650°C, but mass loss was rapid in 650-900°C as it dropped to 75% in this range. It was reported that mass loss in siliceous aggregate concrete was not high and it dropped to only 97% at 1000°C.

(Lie and Kodur 1996) investigated the mass loss of steel fiber reinforced conventional NSC made of siliceous and carbonate aggregates at elevated temperatures. Mass loss was measured using thermogravimetric analyzer in room temperature to 1000°C. It was found in this study that mass loss in concrete was small up to 600°C where only 3% mass was lost. However, mass was lost considerably up to about 30% of in 600-800°C in carbonate aggregate concrete, which was attributed to dissociation of dolomite in carbonate aggregate. However, in siliceous aggregate concrete on 3-4% of mass was lost in entire temperature range of 20-1000°C. It was also found that mass loss of concrete is not significantly affected by presence of steel fiber reinforcement in concrete in entire temperature range.

(Kodur and Sultan 2003) measured the mass loss in plain and steel fiber reinforced HSC in temperature range of 0-1000°C. Mass loss was measured using thermogravimetric analyzer (TGA) up to 1000°C. The mass loss siliceous and carbonate concrete both was very minor upto 600°C, where it was about 3% of the original mass. The mass of carbonate aggregate concrete between 600 and 700°C dropped significantly with the change in temperature. The mass loss again decreased slowly with change in temperature above 750°C. The significant mass loss and density decrease for carbonate aggregate concrete was attributed to the dolomite dissociation in the concrete.

2.2.2.3 Summary

The important thermal properties like specific heat, thermal conductivity, mass loss, and thermal expansion are looked-for envisaging the temperature profiles besides spalling in concrete structures due to exposure to fire. The review indicates that limited observations on NSC are available that exhibits the thermal properties influence on structural members fire resistance. However, there is limietd data on these properties for latest types of HSC (HSC, SCC and FAC). In order to predict the temperature rise in concrete members as well as fire

induced forces, high temperature thermal properties specific to concrete type are to be determined which is one of the main objectives of this research.

2.2.3 Mechanical properties

2.2.3.1 General

In fire resistance designinig the more influencing mechanical properties are compressive strength, elastic modulus, stress-strain response in compression and tensile strength. At elevated temperatures extensive studies are available as for as mechanical properties of concrete are concerned as compare to thermal properties. Elevated temperature mechanical properties at small level are generally tested on typical cylinders or cubes of concrete of variying sizes. The elevated temperature mechanical properties are computed on a wide range of samples sizes due to absence of testing standards unlike room temperature property measurements, where there are specified specimen sizes as per standards. The cylinder specimens of size 75x150, 100x200, and 150x300 mm whereas cube specimens of size 100x100, 150x150 and prism specimens of size 100x300 are used for high temperature.

The primary difference between HSC and NSC in relation to the compressive strength referring to the maximum resistance of a concrete sample to applied pressure. Though precise point of separation between NSC and HSC is not there, however concrete having a compressive strength more than 70 MPa is considered as HSC (Kodur and Harmathy 2008).

Water-cement ratio, curing conditions, aggregated-paste interface transition zone, admixture types and type of stress, aggregated type and size are the main factors on which compressive strength depends upon (Mehta and Monteiro 2006). The compressive strength of concrete is much more than tensile strength, so cracks can propagate easily under tensile loads. Generally, the practice in vogue, tensile strength of concrete is neglected in strength calculations at room as well as at elevated temperature. However, tensile strength of concrete under fire conditions

can be crucial specially in cases where in a HSC structural member fire induced spalling occurs. Also tensile strength is an significant property, as cracking in concrete is normally due to tensile stresses and microcracking progression often generates the structural damage of the member in tension.

Modulus of elasticity of concrete is another property that effects fire resistance and it decreases with temperature. Disintegration of hydrated cement products and breakage of bonds in microstructure of cement paste reduces elastic modulus at elevated temperature and the degree of reduction depends on high temperature creep, type of aggregate and moisture loss.

The compressive stress-strain behavior of concreteat at elevated temperature is significant in the fire resistance analysis of RC structural members. These stress-strain curves at high temperature are supportive to pridict the structural members response under fire. The concrete stress-strain response at high temperature is reliant on factors like curing conditions, aggregate-paste interface transition zone, aggregated size and type. The type of aggregate has a substantial effect on the attained strain in HSC ultimately, on exposure to fire; siliceous aggregate HSC attains lower peak strains as related to carbonate aggregate HSC (Cheng et al. 2004).

2.2.3.2 Previous studies on mechanical properties

There have been significant test programs for characterizing elevated temperature mechanical properties of concrete. In the elevated temperature property tests, the response is measured while specimens are hot at a target temperature. Such high temperature tests (both stressed and unstressed) were carried out by limited researchers to measure the mechanical response (Castillo and Durrani 1990) ;(Lie 1992; Lie and Kodur 1996). However, research on high temperature properties was mostly done through residual property tests after exposure to high temperatures (Chen and Liu 2004)(Chen and Liu, 2004; (Felicetti and Gambarova 1998). Some

of the notable studies on elevated temperature mechanical properties are presented in the following section.

2.2.3.2.1 Compressive strength

Compressive strength of concrete is influenced by aggregate type and size, curing conditions, water-cement ratio, aggregate-paste interface transition zone, type of stress and admixture types (Mehta and Monteiro 2006). Both for NSC and HSC enough studies are available on compressive strength of concrete at high temperatures (Castillo and Durrani 1990). Some noteworthy studies are presented here engendering info on compressive strength of concrete at elevated temperature.

Carette (Painter 1982) studied the use of pozzolans in NSC at high temperatures. They stated that slag and fly ash addition in NSC, after exposure to elevated temperatures did not improve the residual compressive strength of concrete. There was no effect of change in water-cement ratio of NSC with these pozzolans on mechanical properties behavior of concrete at high temperature.

(Lie and Kodur 1996) explored NSC strength properties using steel fibers at high temperature. Researchers noted the degradion of compressive strength of steel fiber RC at a considerable elevated rate with temperature as compared to concrete not having steel fibers. They also discoverd that type of aggregates does not effect the compressive strength significantly.

(Chan et al. 1999) examined the residual compressive strength of both HSC and NSC after introduction to elevated temperatures. He specified three different ranges of temperature namely, 20 - 400°C, 400 - 800°C, and 800 - 1200°C which have diverse effect on loss of compressive strength of concrete. He testified that in 20-400°C the strength loss was comparatively less (upto 10% for HSC and 15% for NSC), however major loss occurred in 400 - 800°C range. Calcium silicate hydrate (C-S-H) gel deterioration and cementing ability due to

dehydration in concrete attributed to this major loss in 400-800°C range. They observed the 400 - 800°C temperature range for concrete as critical strength-loss range. The residual strength above 800°C was observed as only a minor fragment of original strength.

Li et al. (2004) observed the residual mechanical properties of HSC and NSC at high temperatures experimentally. They examined the temperature effects, specimen size, water content, strength grade and profiles of temperature on mechanical properties. They also observed the drop of compressive strength of HSC after 200°C temperature. In HSC the strength loss was higher (36.8%) in 20 - 400°C as observed in NSC (28.8%). Dense microstructure and impermeability of HSC cause the higher loss of strength. They also informed the minimum effect of water content on strength loss of concrete at high temperature. They concluded that loss of compressive strength of larger concrete specimens was lesser than that in reduced size specimens comparatively.

Noumowé (2005) examined the behavior of mechanical properties of plain HSC at high temperature and polypropylene fiber reinforced HSC up to 200°C. He described the higher compressive strength loss of HSC containing polypropylene fibers in comparison to plain HSC.

Sideris (2007) considered the compressive strength characteristics of SCC exposed to elevated temperatures up to 700°C. For comparison, he also verified and equated the results with conventional concretes. Residual strength properties were noticed after exposure to 100, 200, 500, and 700°C. He observed the similarity in trend in residual strength loss of both SCC and conventional concretes in 20-700°C. At temperatures beyond 380°C, both SCC and HSC suffered explosive spalling.

Kim et al. (2009) studied the compressive strength properties of HSC exposed to higher temperatures up to 700°C through stressed test method. During heating, the samples were exposed to a pre-load of 25% of the ultimate compressive strength at room temperature, and

then loaded to failure at 700°C. It was determined by the researchers that as strength of concrete increases, the loss of strength due to raised temperature exposure also increases. It was also determined from this investigation that in 100- 400°C temperature, HSC loses minimum strength but the rate of strength loss is noteworthy beyond 400°C.

The review above shows that comprehensive research on compressive strength properties of both NSC and HSC has taken place for high temperature behavior. However, it can be noticed that consistency is not there in the strength trends for both NSC and HSC and there are noteworthy variations in strength loss, as conveyed by numerous authors. Moreover, inadequate data in literature is available on high temperature strength properties of various types of concrete like SCC, FAC and fiber reinforced HSC. Therefore there is a need to collect the data on strength properties of new types of concretes exposed to elevated temperature for evaluating structural members response made of HSC.

2.2.3.2.2 Tensile strength

Tensile strength of concrete at ambient temperatures can be evaluated through three methods namely, flexural tensile, direct tension, and splitting tensile strength tests. Flexure tensile strength is obtained through subjecting a concrete beam to third-point flexural loading (ASTM C78, 2009). The direct tensile strength is measured by testing cylinder or prism specimens by applying axial tensile load in a suitable test machine until specimen breaks in direct tension (ASTM C1583, 2004). Direct tension test is less reliable as the specimen holding devices (grips) introduce secondary stresses leading to unreliable strength data. In splitting tensile test a compressive load is applied on the generatrices of the specimen which are diametrically opposite (ASTM C496, 2004). The load is increased until failure occurs by splitting of the specimen along the vertical diameter. At ambient temperature, splitting tensile strength is

usually 50-70% greater than direct tension strength, where as it is 40-50% lower than flexure tensile strength (Popovics, 1998).

Compressive strength of concrete, aggregate-paste interface transition zone, microstructure of concrete, water/cement ratio and presence of any flaws are the major factors on which tensile strength of concrete depends upon (Neville, 2004). A review of the literature shows that limited studies are available on tensile strength of concrete at high temperature. It is also worth noticing that all previous studies on tensile strength of concrete at elevated temperature are based on residual strength tests which are applicable for concrete members cooled after exposure to fire. The tensile strength behavior of hot concrete (during fire exposure) cannot be represented by this residual tensile strength property which is required for predicting spalling. Some noteworthy studies are presented here engendering info on tensile strength of concrete at high temperature.

Carette et al. (1982) examined the effect on the tensile strength of NSC at high temperature. He tested concrete cylinders in temperature range of 75-600°C using residual strength technique. He found reduction (65-70%) in splitting tensile strength at 600°C. He determined that type of aggregate as well as water cement ratio have important influence on the splitting tensile strength of NSC.

Felicetti et al. (1996) examined the residual tensile strength of two types of HSC from room temperature to 600°C by testing using direct tension method. They observed reduction in tensile strength to zero at about 600°C. It was also noticed in this study that at high temperature concrete softens and that temperature has a noticeable effect on its tensile strength.

Bahnood and Ghandehari (2009) informed residual splitting tensile strength of plain and polypropylene fiber reinforced HSC up to 600°C. The researchers concluded that the splitting tensile strength decreases due to decomposition of hydrated cement products and thermal

incompatibility between cement and aggregates paste. They also noticed that there was no conspicuous difference in the splitting tensile strength of polypropylene fiber reinforced HSC and plain HSC up to 600°C.

Li et al. (2004) tested for residual splitting tensile strength of HSC in temperature range of 200-1000°C. Cement was replaced by 27 per cent fly ash in HSC batch mix. 100 mm concrete cubes were used to measure splitting tensile for HSC at 200, 400, 800 and 1000°C temperatures. A retained splitting tensile strength of 51.9% at 800°C and 16.9% at 1000°C was reported which is significant at these temperatures. Appearance and propagation of cracks was observed to be more obvious in tensile strength as compared to compressive strength tests. Decrease in splitting tensile strength with elevated temperature was attributed to thermal stresses generated in dense microstructure of HSC that caused in micro and macro cracks.

2.2.3.2.3 Elastic modulus

Elastic influences the structural members at elevated temperature as the modulus of concrete degrades with temperature. Elastic modulus reduces at elevated temperature because of disintegration of breakage of bonds in microstructure of cement paste and hydrated cement products and the range of reduction depends on type of aggregate, elevated temperature creep and moisture loss (Bažant and Kaplan, 1996).

Some of noteable studies carried out on high temperature elastic modulus are discussed below:

(Castillo and Durrani 1990) analyzed the temperature effect on elastic modulus of both HSC and NSC in 20 - 800°C temperature range. Measurement of modulus was done through closed-loop servo-controlled hydraulic testing machine integrated with an electric furnace. The researchers stated that both HSC and NSC have same loss of modulus at high temperature. Minor loss was noticed up to 400°C and quicker loss was noticed between 400 - 600°C.

Progressive dehydration and loss of bond between materials causes the higher loss above 400°C.

(Bamonte et al. 2010) examined HSC and SCC cylinders up to strength of 90 MPa for elastic modulus at 20°C, 200°C, 400°C, and 600°C. They informed that the elastic modulus is comparative lesser in hot state in comparison to residual which was ascribed to thermal affects. It was also determined that there is no variance in the elastic modulus of SCC and HSC.

(Persson 2004) studied experimentally the SCC elastic modulus at raised temperatures and as residual property. He tested at temperatures of 20, 200, 400, 600 and 800°C. He noticed a lower elastic modulus for SCC, as compared to HSC, throughout the temperature range in both hot state and as residual property.

2.2.3.3 Summary

Tensile strength, elastic modulus, compressive strength, and stress-strain curves are central mechanical properties that are required for predicting fire performance of RC structural members. The above review illustrates that good amount of data exists for high temperature mechanical properties for NSC and also limited data exists on HSC. But this data is not available for HSC such as FAC and SCC with and without fibers. This data is desirable especially for high temperature tensile strength, elastic modulus and curves of stress-strain for these HSC. Thus one of the major objectives of this research is to evaluate high temperature mechanical properties for these new types of concrete. The generated test data can be used to develop mathematical relations for various properties as a function of temperature.

2.2.4 Deformation properties

2.2.4.1 General

Deformation properties include thermal expansion, creep and transient strains and these depend on the type of aggregate used, and chemical and physical reactions occurring in cement paste (Schneider 1988).

2.2.4.2 Previous studies

The coefficient of thermal expansion (CTE), defined by change in length of material per degree rise in temperature, is an important measure to measure thermal stresses as a result of temperature variation (Kodur and Harmathy 2008). CTE of concrete depends on type of aggregate, its composition, and moisture content (Dwaikat 2009). The thermal expansion of concrete with siliceous aggregate is considerably more as compared to concrete with carbonate aggregate. Published data plotted in Figure 2.18 shows that CTE varies for different aggregate types.

Creep strain is time-dependent plastic strain under constant stress level. It is associated with the moisture movement inside concrete, therefore, is influenced by the temperature. At elevated temperatures, creep strains are significant since moisture movement occurs more rapidly. Creep strains depends on many factors including temperature, stress levels, time, loading and mix design of concrete (Dwaikat 2009). A review of literature shows that creep strains are significant in low-modulus aggregates. Creep is more pronounced at higher load level and elevated temperatures.

In concrete, transient strain also develops in addition to creep during the first heating under load and is independent of time (Khoury 2000). It is caused by thermal incompatibilities (differential thermal expansion) between aggregate and cement paste (Purkiss 2007). The mismatch in thermal expansion between aggregate and cement paste leads to development of

internal stresses and micro-cracking and this results in transient strains to occur in concrete (Schneider 1988). Currently, limited information is available in the literature on high temperature creep and transient strains (Kodur and Harmathy 2008). Constitutive relationships for high temperature creep and transient strains of concrete have been developed by Anderberg and Thelandersson (Anderberg and Thelandersson 1976) and Harmathy (Harmathy 1993), and is given by these two equations:

$$\varepsilon_{cr} = \beta_1 \frac{\sigma}{f_{c,T}} \sqrt{t}\, e^{d(T-293)} \quad \text{(Anderberg model)} \qquad 2.1$$

$$\varepsilon_{tr} = k_2 \frac{\sigma}{f_{c,20}} \varepsilon_{th} \quad \text{(Harmathy model)} \qquad 2.2$$

where ε_{cr} = creep strain, ε_{tr} = transient strain, $\beta_1 = 6.28\times10^{-6}$ s$^{-0.5}$, $d = 2.658\times10^{-3}$ K^{-1}, T = concrete temperature (K) at time t (s), $f_{c,T}$ = concrete strength at temperature T, and σ = stress in the concrete at the current temperature, k_2 = a constant ranges between 1.8 and 2.35, ε_{th} = thermal strain, and $f_{c,20}$ = concrete strength at room temperature.

These equations generally produce reasonable estimates for high temperature creep and transient strains in concrete.

Deformation properties of concrete include creep and transient strains and are mainly influenced by strength, aggregate type, sustained stress and chemical and physical reactions that take place in concrete under fire conditions (Schneider, 1988). Creep is the time-dependent plastic strain under continuous stress and temperature. At room temperature sustained external stress becomes the driving force for the movement of the physically absorbed water and water held in small capillaries (Mehta and Monteiro, 2006). Due to limited moisture movement in concrete at room temperature, creep deformations are slow to occur. However, at elevated temperatures, moisture movement is usually significant in concrete that leads to higher creep strains. High temperature creep strains are thus largely influenced by concrete temperature

(Dwaikat, 2009). Because high temperature creep affects strains, deflections, and stress redistribution at elevated temperatures, it plays an important role on the fire resistance of structural members.

Transient strain on the other hand occurs during the first time heating of concrete, but it does not occur upon repeated heating (Khoury et al., 1985). Transient strain is independent of time and is essentially caused by the thermal incompatibilities between the aggregate and the cement paste (Purkiss, 2007). Exposure of concrete to high temperature induces complex changes in the moisture content and chemical composition of the cement paste. Moreover there exists a mismatch in thermal expansion between the cement paste and the aggregate. Therefore factors such as changes in chemical composition of concrete and mismatches in thermal expansion lead to internal stresses and micro-cracking in the concrete constituents (aggregate and cement paste) and results in transient strain in the concrete (Schneider, 1988).

2.2.4.3 Summary

High temperature creep and transient strain of concrete are complex phenomenon and are influenced by factors such as temperature, strength, moisture content, loading, and mix proportions. The creep deformation generally increases with temperature, with low-modulus aggregates (Schneider 1988) and also with increasing load levels at elevated temperatures. Transient strain is independent of time and does not recur as it is encountered only in first heating of concrete.

2.3 Reinforcing steel

The behavior of reinforcing steel has been extensively studied and a comprehensive review is given by (Lie 1992)and (Khoury 2000)

2.3.1 Thermal properties

Thermal properties of steel at elevated temperature include thermal conductivity and specific heat (thermal capacity). The steel type and type of fire exposure defines the thermal behavior of steel reinforcement. The heat transfer through steel is very rapid as compared to concrete due to high conductive characteristics of steel reinforcement. At room temperature, thermal conductivity may vary slightly depending on the chemical composition of steel (Bisby 2003). However, at elevated temperature, thermal properties are more dependent on temperature and are less influenced by the steel composition (Williams 2004a).

Thermal conductivity decreases linearly with increasing temperature up to about 900$_o$C and thereafter remain constant at elevated temperatures (Lie 1992) Figure 2.12 (a) shows the variation of thermal conductivity of reinforcing steel with temperature. Specific heat, defined as amount of heat required to raise the temperature of unit mass by unit degree, varies with temperature. The peak in specific heat around 700$_o$C can be attributed to phase transformation. The steel reinforcement area is very small in comparison to overall concrete section and also reinforcing steel is located within the concrete section; therefore, steel has almost no influence on temperature distribution within concrete cross section.

2.3.2 Mechanical properties

The mechanical properties that influence fire response are yield strength, ultimate strength, elastic modulus and stress-strain relationship. Literature review suggests that there is considerable variation in yield and ultimate strength of steel since these properties depend on steel composition and the definition of yield strength. (Buchanan 2002). Stress-strain curves for mild steel at various temperatures are shown in Figure 2.12. It can be seen that the yield strength decreases with temperature and well defined yield plateau disappears at higher temperatures. Figure 2.14 shows that elastic modulus, yield and ultimate strength of reinforcing steel decreases n with temperature. The reinforcing steel recovers nearly all of its original yield

strength upon cooling as long as heating temperatures do not exceed 500°C (Neves et al. 1996). Eurocode assumes that reinforcing steel maintain its room temperature strength up to 400$_o$C. Type of fire exposure is an important factor to be considered in evaluating fire resistance of RC members. Concrete and reinforcing steel recover some of its strength and stiffness during decay (cooling) phase of design fires (non standard fire). The amount of recovery depends on the highest temperature recorded in reinforcing steel. Reinforcing steel heated above 500$_o$C experience a gradual decrease in residual strength. Therefore, the behavior of reinforcing steel in the cooling phase is critical for modeling the response of FRP-strengthened RC structural members exposed to real (design) fire scenarios.

2.3.3 Deformation properties

Thermal elongation and creep strain are the deformation properties of steel. The thermal elongation of steel is quantified through coefficient of thermal expansion (CTE) that indicates thermal strain induced per degree rise of temperature. In general, CTE of reinforcing steel increases with temperature except between 650 to 815$_o$C where it decreases due to molecular transformation in steel. Thereafter, it increases again as shown in Figure 2.15.

Creep is time dependant increase in plastic strain under constant stress. This is an important property of reinforcing steel that has significant influence on behavior of RC members under fire conditions (above 450$_o$C). Thus, creep should be included in numerical modeling to evaluate fire performance of structural member (beam). Limited information is available in the literature about creep strain variation with temperature for steel reinforcement. The available creep models, such as the one proposed by (Harmathy and Research 1967), are based on Dorn's theory, which relates the creep strain to the temperature, stress, and time.

2.4 Codes and standards

The specifications for fire resistant design are included in building codes and national standards of various countries. These provisions are usually prescriptive in nature, as the codes and standards provide tabulated values of fire resistance which are based on standard fire tests. These tabulated fire resistance values are mostly dependent on concrete cover thickness and minimum dimensions of structural members.

In the USA, concrete structures are designed in accordance with the American Concrete Institute (ACI-318) (2008) standard. While ACI-318 does not contain any fire provisions, it refers to ACI 216.1 (2007) standard which gives prescriptive based specifications for fire design of concrete and masonry structures. ACI 216.1 standard specifies concrete cover thickness and minimum sectional dimensions required for achieving a desired fire resistance rating in RC columns. Similarly, Eurocode 2, Part 1–2 (2004) gives simplified approach for determining fire resistance of RC columns based on tables and advanced methods. For example, to reduce fire induced spalling; Eurocode suggests a reinforcement mesh with a nominal cover of 15 mm to HSC columns.

It can be seen that these provisions provide prescriptive approaches based on experimental studies. Tables, which are based on this approach, provide the faster and most direct method for determining the minimum dimensions and cover thickness in RC columns. The simplified equations may give more economical fire resistant designs, especially for small columns and/or high fire resistance periods. However, the important factors such as HSC, use of different combination of fibers and effect of tie configuration are not comprehensively taken into account by these standards.

2.5 Summary

Based on information presented in this chapter, it is evident that high temperature material properties are crucial for modeling the fire response of RC members. Good amount of data exists on high temperature thermal, mechanical and strength properties including elastic modulus of NSC and to some extent for HSC as well. However, there very limited property data on HSC (HSC, SCC, FAC) is available at elevated temperatures. It is also established that mostly the fire resistance tests were conducted on RC columns made of NSC and HSC, but these tests are not existent for HSC columns such as FAC and SCC. Moreover, limited data is available on effect of hybrid fibers on spalling mitigation in HSC columns. Further, the guidelines put forward by experimental studies have not been fully incorporated in numerical models. Important factors such as high temperature material properties of HSC, use of hybrid fibers, and effect of tie configuration are not fully incorporated in numerical models.

FIGURES OF CHAPTER 2

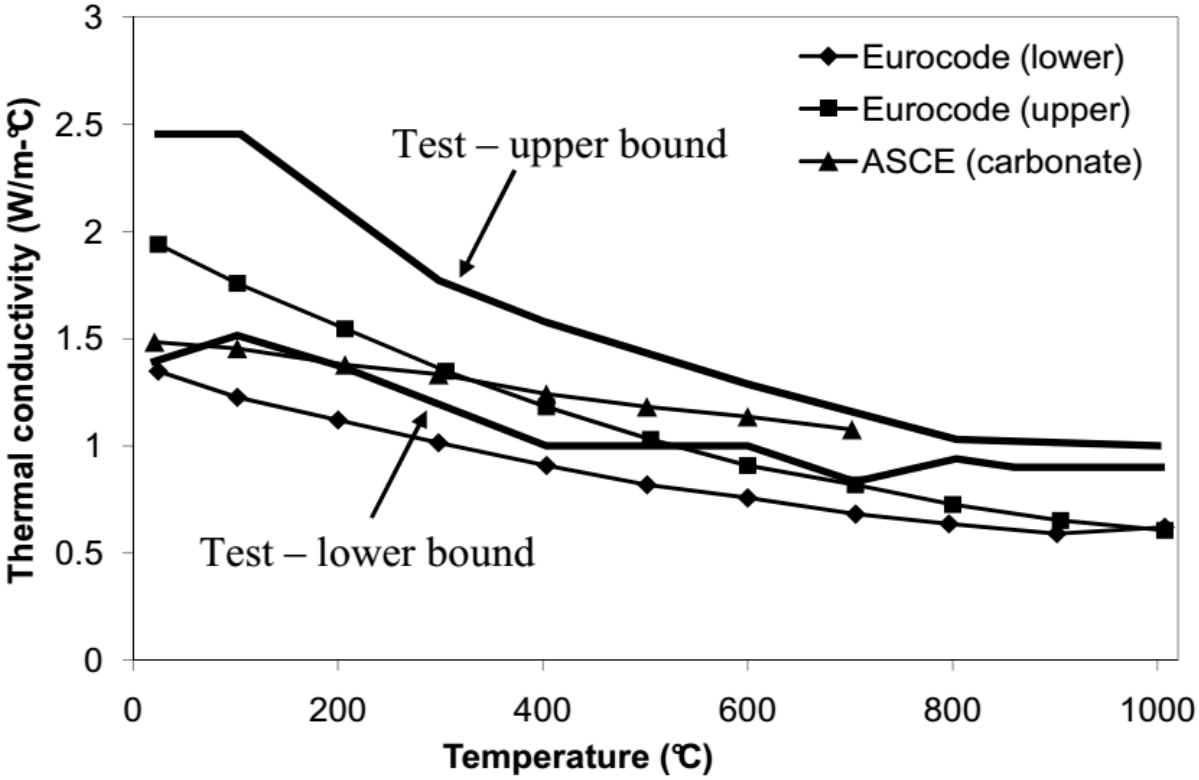

Figure 2.1 Variation in thermal conductivity of NSC as a function of temperature

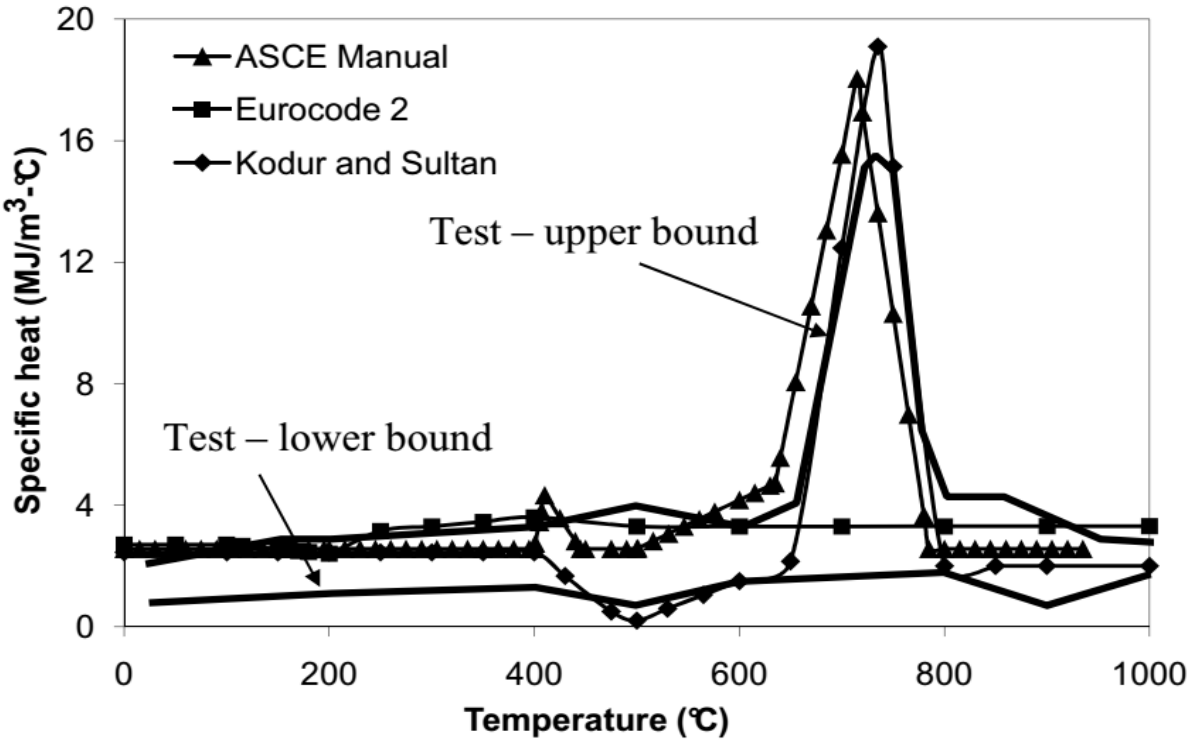

Figure 2.2 Variation in specific heat of NSC as a function of temperature

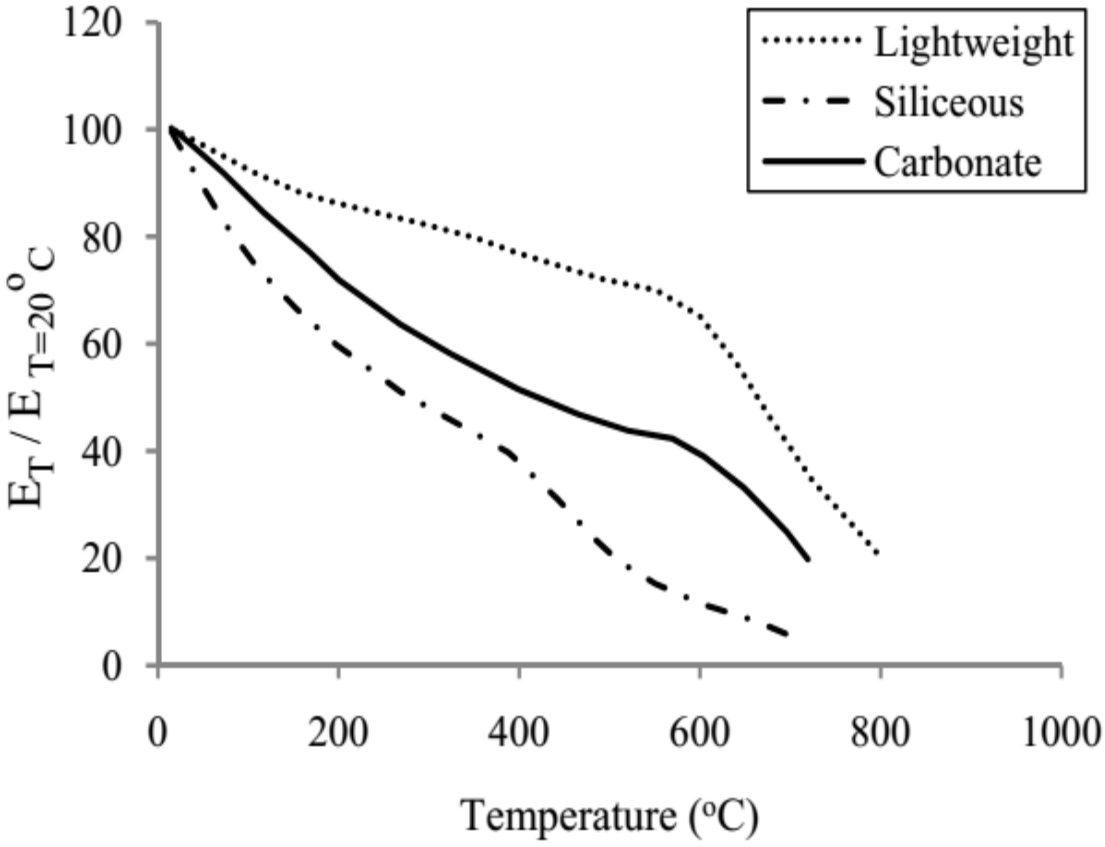

Figure 2.3 Elastic modulus changes of concrete as function of temperature

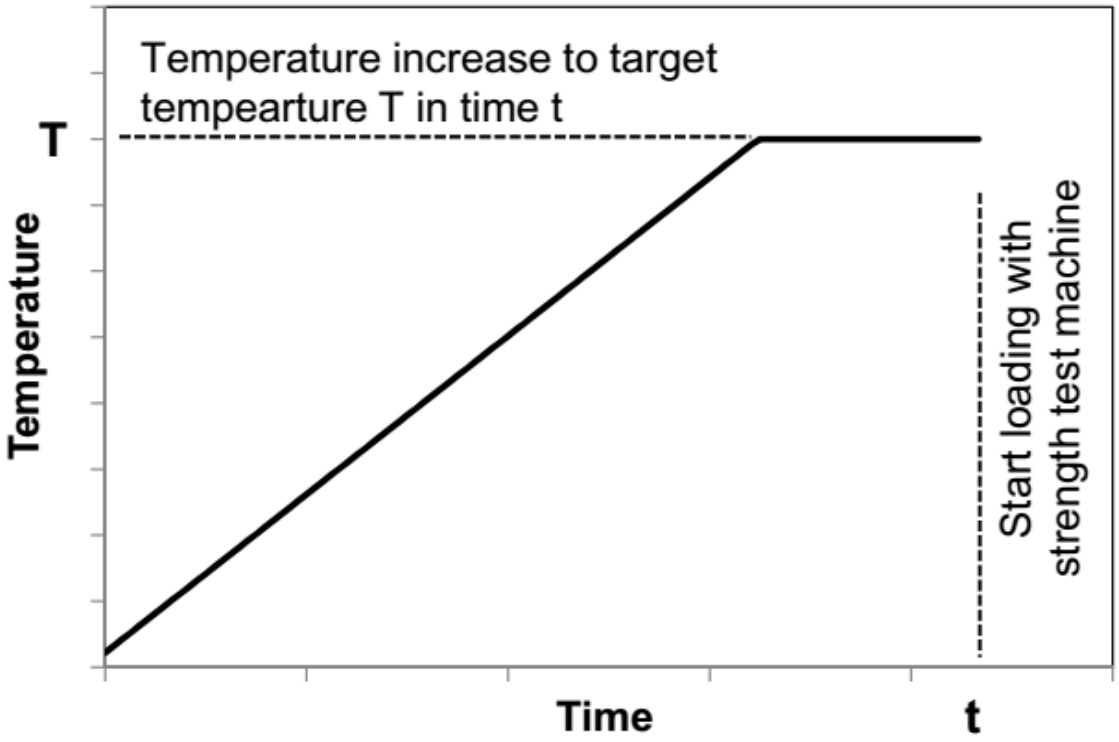

(a) Heating scheme

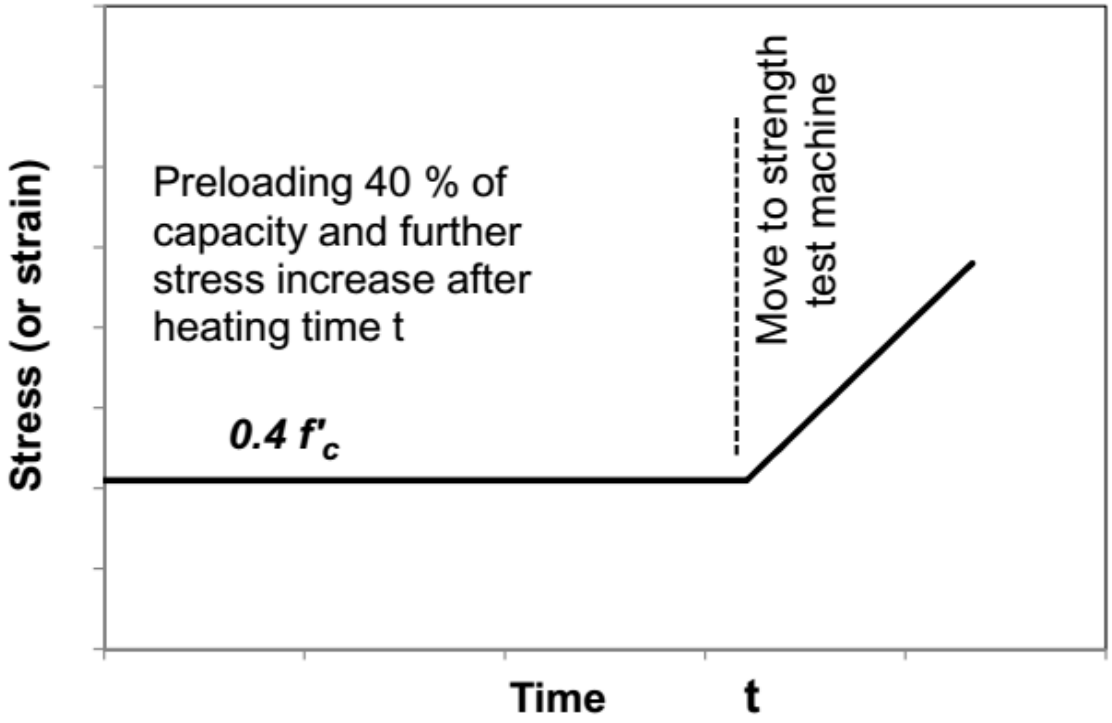

(b) Loading scheme

Figure 2.4 Specimen heating and loading in stressed test method under preload

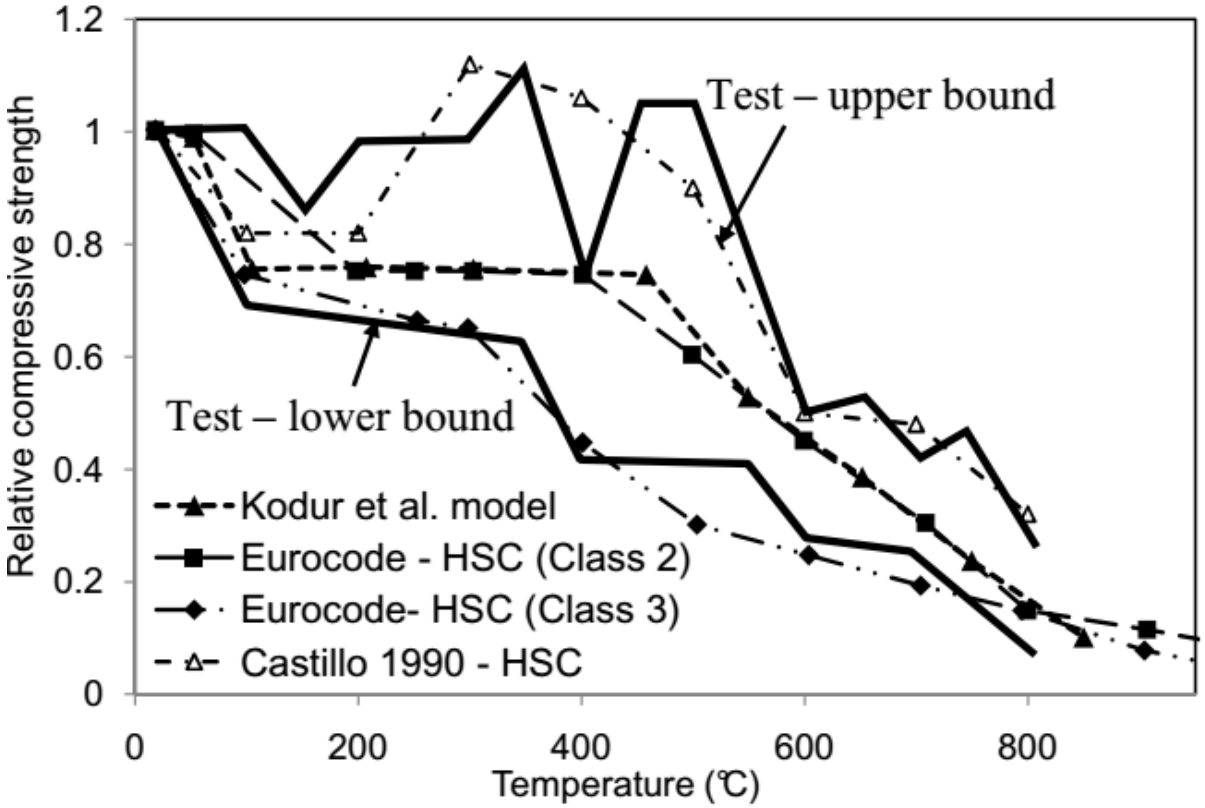

Figure 2.5 Change in relative compressive strength as a function of temperature for HSC

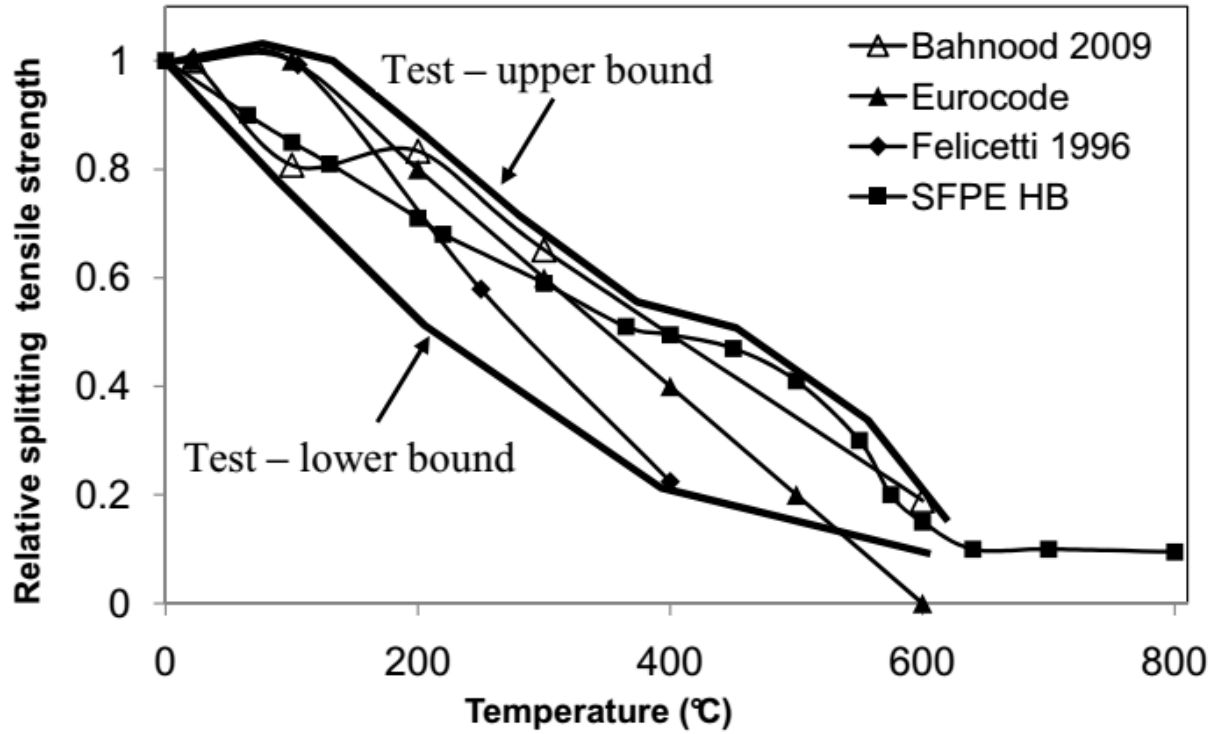

Figure 2.6 Change in relative splitting tensile strength as a function of temperature

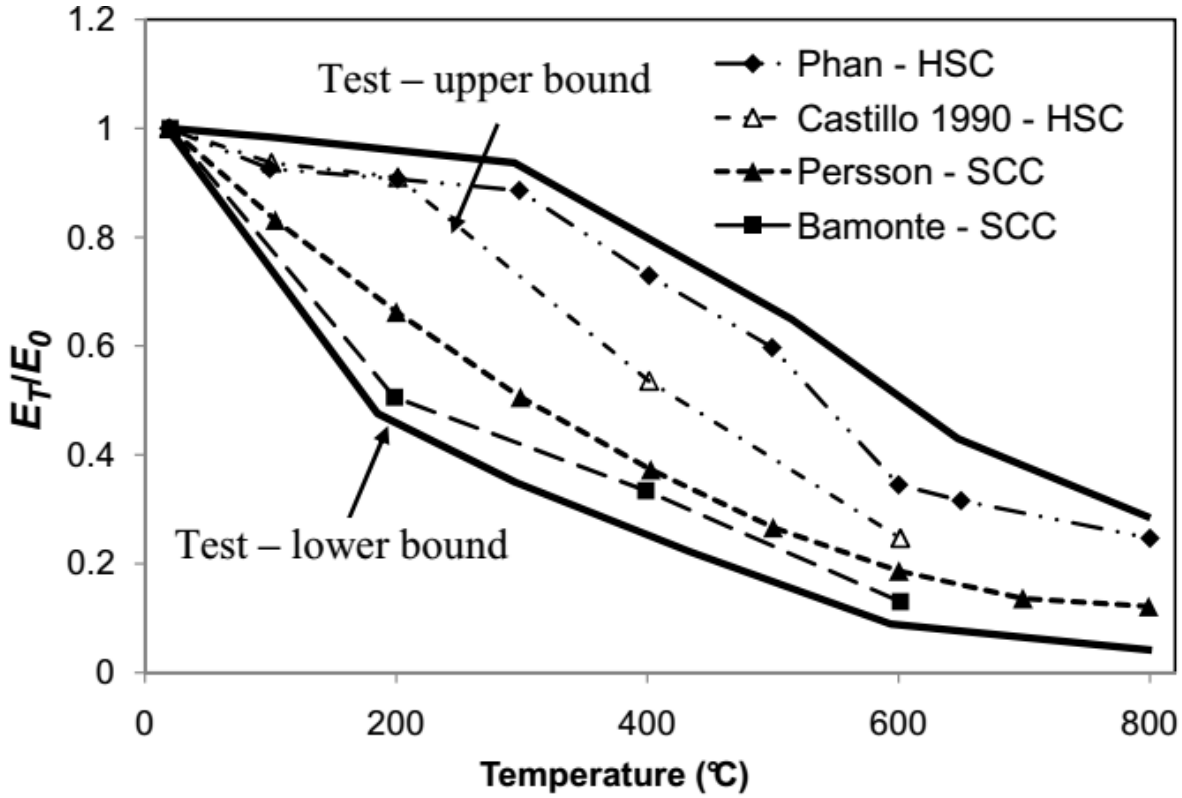

Figure 2.7 Variation in elastic modulus as a function of temperature

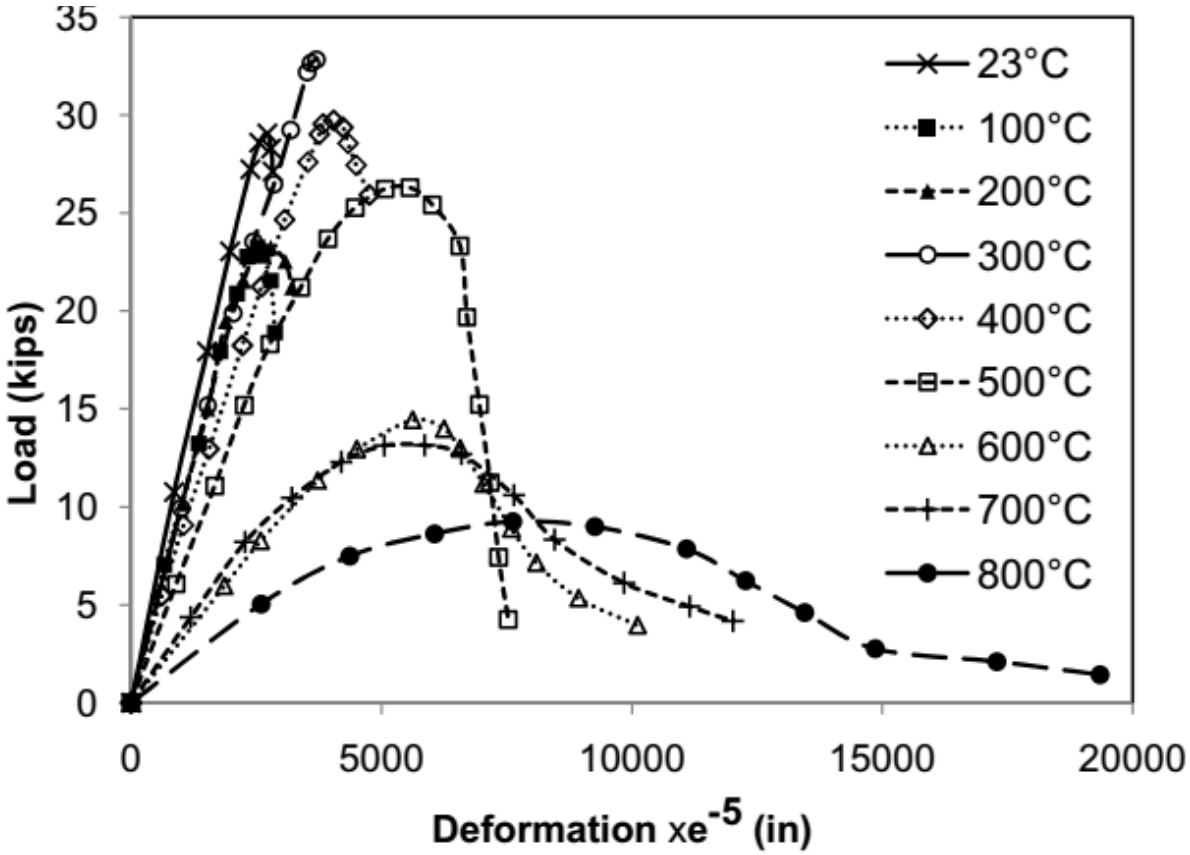

Figure 2.8 Typical load deformation of HSC at various temperatures

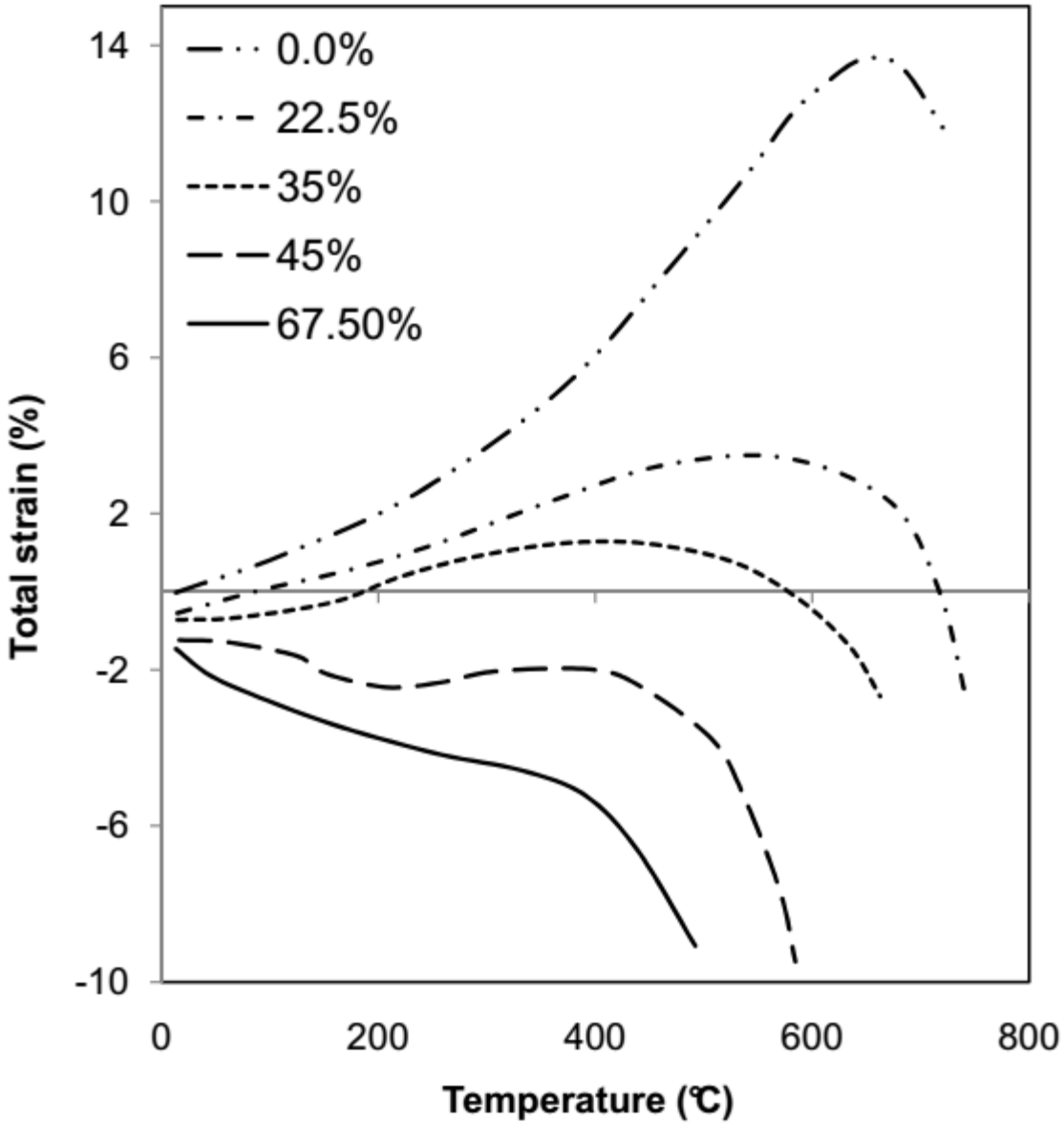

Figure 2.9 Variation of total strain with temperature for concrete heated under differnet preloads (Anderberg and Thelandersson 1976)

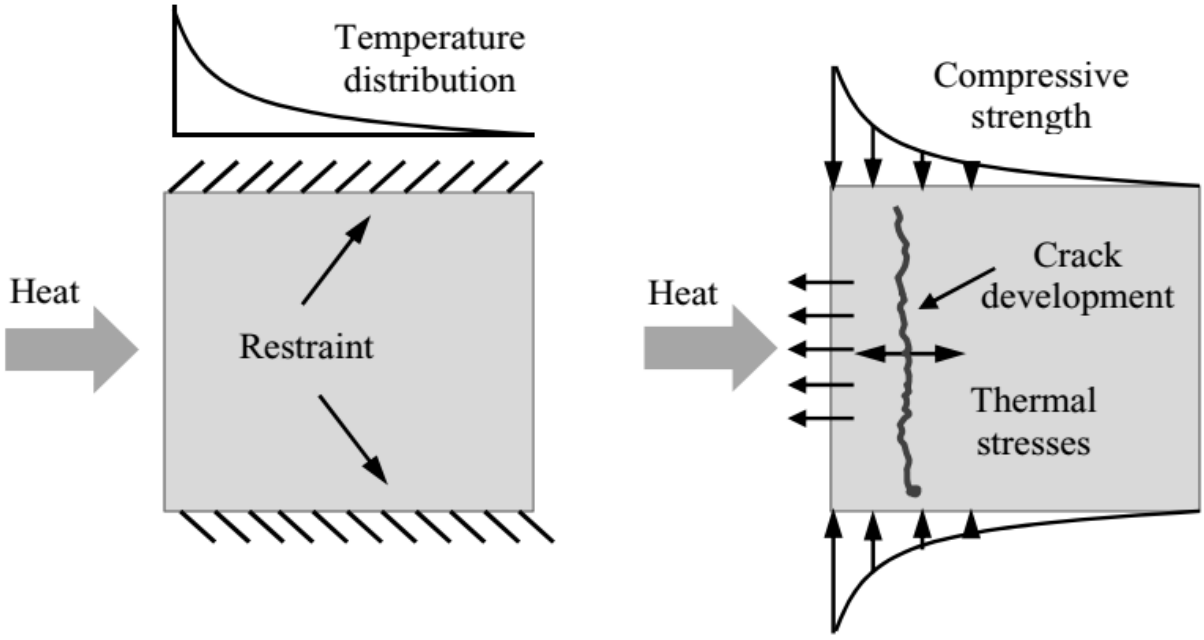

(a) Restrained concrete (b) Developed stresses

Figure 2.10 Illustration of thermal dilation mechanism for fire induced spalling

CHAPTER – 3

ADDITION OF MATERIAL IN OPENSEES MATERIALS LIBRARY AND ITS VALIDATION

3.1 General

Modelling of structures using subjected to dynamic static and static loads (e.g. wind, snow, , earthquake and impact) using finite-element software are very common and extensively being used in construction industry. However, to study the structure response of fire, modelling which is highly tedious, the full (often coupled) sequence of a realistic fire scenario, heat transfer to structure and structural response is required and only a few of the top consulting engineers in the world truly specialize in this niche area.

OpenSees is full form of Open System for Earthquake Engineering and Simulations, a powerful program written in object oriented language C++. Frank McKenna is developer of OpenSees. OpenSees is not a code, it's a robust tool which can perform nonlinear incremental dynamic analysis and performance based design with less effort and time because of the coding loops that can be made.

3.2 Why OpenSees

It consists of wide variety of material models and one can also customized one's own material, and its ever growing library. It has numerous options to define the element from elastic to non-linear, from lumped plasticity to concentrated plasticity and from force based to displacement based. Intricate linear or nonlinear structural and geotechnical modeling can be done. It is very robust tool for simulations capable of performing static pushover, static reversed cyclic, dynamic time history analysis, and uniform support excitation, multi support excitation and incremental dynamic analysis.

3.3 Modified material classes / coding in OpenSees

Different types of material models are available in OpenSees for concrete and steel, which define their mechanical constitutive relation, however, few of them required to be improved to include properties dependent upon temperature. In this thesis temperature dependence will only be incorporated to the unixial material models because the reliable data is not available for the multiaxial material models. Eurocode based stipulations will be primarily The uniaxial properties at elevated temperature on.

Two classes <Concrete02Thermal> and <Steel01Thermal> are created which are temperature dependent. Uniaxial material classes <Concrete02> and <Steel01> are modified to create <Concrete02Thermal> and <Steel01Thermal> in OpenSees by Jiang, J. etal. These new material classes hierarchy is shown in Figure below.

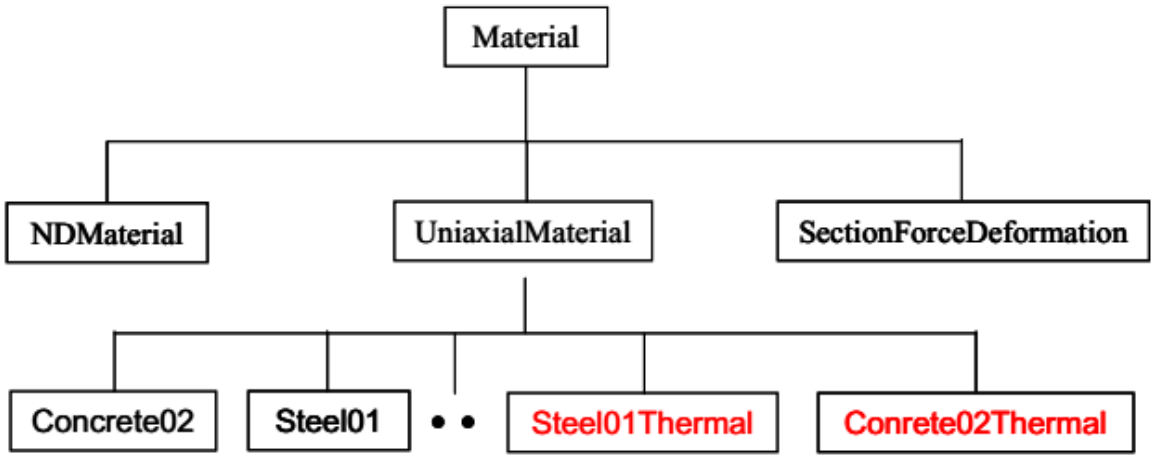

Figure 3.1 Modified material class in OpenSees

3.4 Thermal properties

The material class <Concrete02Thermal> has been further modified for high strength concrete into OpenSees materials library.

The relations of thermal property are proffered with respect to different temperature ranges in Table 3.1.

Table 1.1 Relationship of thermal properties with respect to different temperature ranges (Khaliq and Kodur 2011)

Properties	Type of Concrete	Equation
Thermal conductivity (W / m-°C)	HSC	k_t = 3.12-0:0045T 20°C≤T≤400°C; 3-0:0025T 400°C≤T≤800°C
Specific heat (MJ/m^3-°C)	HSC	cp = 2.4 + 0.001T 20°C≤T≤400°C; 0.6-0.006T 400°C≤T≤800°C
Thermal expansion (%)	HSC	εth = 0 20°C; -0.1 + 0.0015T 20°CbT≤800°C
Compressive strength	HSC	βT , compression = 1.0 20°C; 0.99-0.002T 100°C≤Tb200°C; 0.73-0.0005T 200°C≤T≤800°C
Splitting tensile strength	HSC	βT , tensile = 1.0 20∘C; 0.99-0.001T 100°C≤T≤800°C
Elastic modulus	HSC	βT , modulus = 1.0 20°C; 0.84-0.001T 100°C≤T≤800°C
Thermal conductivity (W/m-°C)	HSC	k_t = 3.12-0:0045T 20°C≤T≤400°C; 3-0:0025T 400°C≤T≤800°C

3.5 Mechanical properties

Single representative relation is expressed for f_c',T as there is least variation in compressive strength of SCC at elevated temperature,. However, there is significant difference in elastic modulus and splitting tensile strength variation at elevated temperatures, so separate equations are there for SCC.

$$\beta_{T,compressive} = f'_c,T / f'_c$$

$$\beta_{T,tensile} = f'_t,T / E_c$$

$$\beta_{T,modulus} = E_c,T / f'_c$$

Table 3.2 Reduction factor (βT) of elastic modulus, tensile strength and compressive strength with respect to various temperatures of SCC

Temperature °C	Factors of Reduction (βT)		
	Elastic modulus	Tensile strength	Compressive strength SCC
20	1	1	1
100	0.74	0.95	0.79
200	0.64	0.9	0.59
300	0.54	0.8	0.56
400	0.44	0.7	0.53
600	0.34	0.5	0.43
800	0.04	0.3	0.33

Conventionally, concrete tensile strength should usually be ignored. The tensile strength reduction $f_{ct,T}$ of a concrete at high temperature is defined by the reduction factor

$k_{ct}=f_{ct,T}/f_{ct}$, it is stated as

For $20^oC \leq T \leq 100°C$

$$k_{ct} = 1$$

For $100^oC < T \leq 600°C$

$$k_{ct} = 1 - \frac{T - 100}{500}$$

The concrete thermal elongation strain ε_{cth} can be found as follows:

Siliceous aggregates:

For $20^oC \leq T \leq 700°C$:

$$\varepsilon_{cth} = -1.8x10^{-4} + 9x10^{-6}T + 2.3x10^{-11}T^3$$

For $700^oC < T \leq 1200°C$:

$$\varepsilon_{cth} = 1.4x10^{-2}$$

Calcareous aggregates:

For $20^oC \leq T \leq 805^oC$:

$$\varepsilon_{cth} = -1.2x10^{-4} + 6x10^{-6}T + 1.4x10^{-11}T^3$$

For $805^oC < T \leq 1200^oC$:

$$\varepsilon_{cth} = 1.2x10^{-2}$$

3.6 Benchmark testing of developed codes in OpenSees

The key features of structures in fire are presented first followed by the analytical solutions of the deflection and reaction force of an individual beam subjected to different boundary and thermal load conditions. These analytical solutions are derived to judge the performance of the developed OpenSees when temperature independent linear elastic material is used. In the developed OpenSees is used to analyze the behavior of a single beam under fire conditions. In these cases a temperature dependent elastic material is used and the OpenSees results are compared with the examples given in the already studies carried out.

In this work HSC has been incorporated with and without fibers into the existing material library of OpenSees. The method used to incorporate the new material (HSC) is attached as Appendix B. The amended Code used for HSC is attached as Appendix A.

Geometric properties of cross section used in validation of the incorporated material is shown in Table 3.3 and the drawing is shown in Fig. 3.23. The comparison of beam deflection under temperature loading is shown in Fig. 3.24. Result shows the complete conformity with the practical example.

Table 3-2 Geometric properties of cross section applied in testing

Property		**Nomenclature / Dimension**
Cross section (mm)		400 x 600
Length (m)		5 m
Reinforcement	Top bars (# 5 grade 60 bars)	2 x 15.8 mm
	Bottom bars (# 8 grade 60 bars)	4 x 25 mm
f'_c (N/mm^2)		90 MPa
f'_y (N/mm^2)		414 (Grade 60)
Applied total load (kN/m)		60
Bottom concrete cover thickness (mm)		50
Top concrete cover		40
Support condition		SS
Fire type		ASTM E119

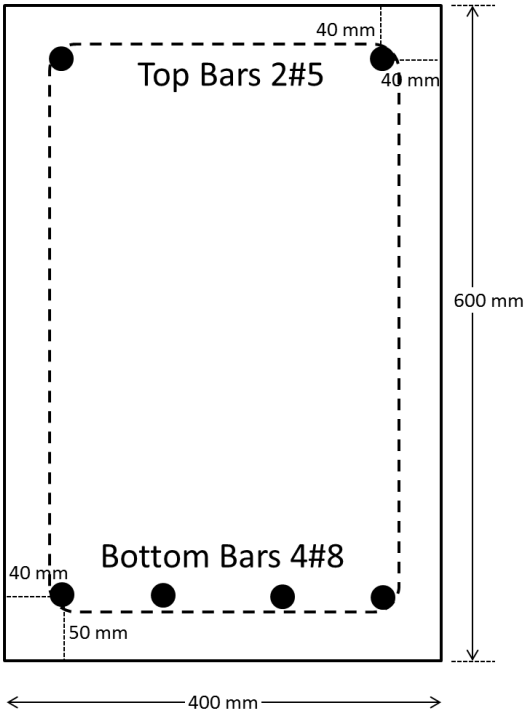

Fig. 3.23 cross section of validation beam

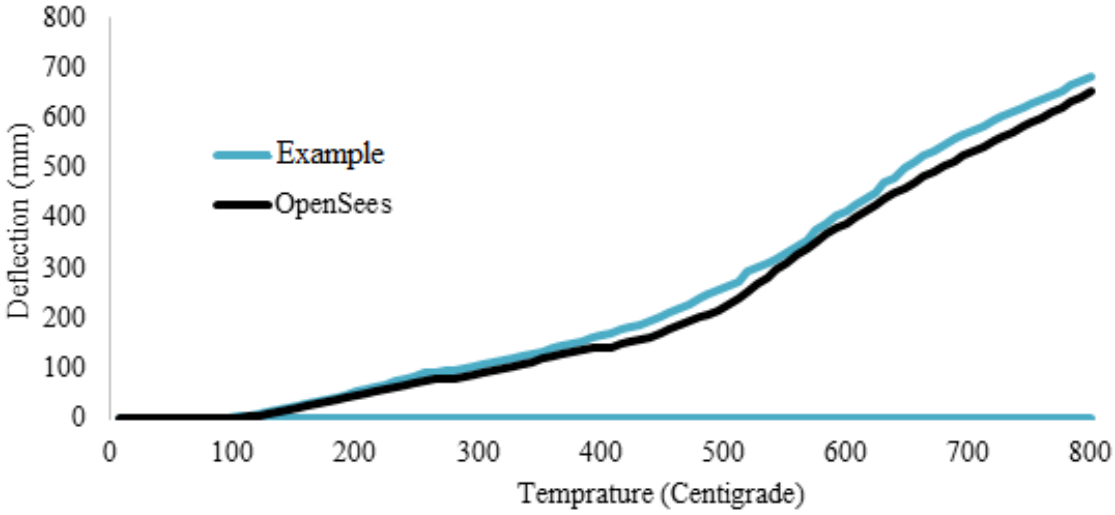

Fig. 3.5 Validation of newly incorporated material class in OpenSees

CHAPTER 4

THERMOMECHANICAL ANALYSIS OF BEAM STRUCTURES USING OPENSEES AND DISCUSSION

4.1 General

There are few experimental studies on the fire resistance of RC beams. Further, most of the experimental studies were done under 'standard' conditions that did not cover significant features like the axial restraint and fire scenario, which will affect the fire response of RC beams. For these reasons, beams were modelled on NSC and HSC beams in ASTM standard fire, axial restraint, and loading conditions. Two of the beams were modelled under standard fire exposure. The other four beams were modelled under typical design fire scenarios. A significant amount of data was collected and analysed. Details of the results are presented in this chapter and the different parameters are analyzed.

4.2 Modelled specimens

The six RC beams were modelled in Opensees for fire resistance tests designated B-l to B-6. Out of these four beams, B-3, B-4, B-5 and B-6, were made of HSC. The other two beams, B-l and B-2, were of NSC. Length of all beams was 3960 mm and rectangular cross-section was of 406 x 254 mm. These beams were designed as per ACI318 specifications (2008). A summary of the test parameters and results for these beams are given in Table 4.1.

The beams were designed with 3 ϕ 19 mm bars as main tensile reinforcement and 2 ϕ 13 mm bars as compressive reinforcement. The shear reinforcement consisted of ϕ 6 mm stirrups spaced at 150 mm over the length of the beam and bent at 135° into the concrete core. The steel used for the main reinforcing tensile bars and stirrups had detailed yield strengths of 420 MPa and 280 MPa, respectively. Figure 4.1 shows the elevation and cross-sectional drawings of the

beams, together with the location of the stirrups. In each beam, the bars were tied with the stirrups to form a steel cage as shown in Figure 4.2.

4.3 Test Results

Data produced from the tests above of fire modelling was utilized to assess the fire behaviour of RC beams under various circumstances. The test model variables encompassed axial restraint, concrete strength, load level, and type of fire exposure. The assessment is done by relating the structural response, thermal response, and failure forms in addition to fire resistance time.

4.4 Thermal response

The thermal response of HSC and NSC beams obtained in analysis is shown in Figures 3.9 and 3.10 by drawing concrete temperatures and rebar as a function of exposure time to fire. While beams B-l and B-3 were modelled as exposed to ASTM El 19-standard fire (no decay phase) as shown in Figure 4.8, beams B-2 and B-4 were modelled to a short design fire, with a definite decay segment as shown in Figure 4.9. The temperature plateau may be primarily attributed to the water evaporation in concrete which consumes a noteworthy amount of energy. Next to the plateau, the temperatures in the concrete and rebar increase with exposure of fire time. These figures also show that the temperatures measured in concrete decrease with distance increasing from the bottom surface. This is attributed to the low thermal conductivity and high thermal capacity of concrete which decreases heat penetration towards the inner layers of concrete. The temperatures plotted in Figures 3.9 and 3.10 may be used to measure the effect of concrete strength on the thermal response of HSC and NSC beams. The HSC and NSC beams had similar characteristics except for the strength, and were exposed to comparable load levels. This can be observed from Figure 3.8 that the temperatures measured in rebars and concrete (at 100 mm concrete depth) in the NSC beam (B-l) are lesser than the corresponding

temperatures in the HSC beam (B-3) throughout the exposure to fire. The variation in profiles of temperature can be partially attributed to variances in thermal properties of the two concretes resulting from higher density (lesser porosity) of HSC and attruibuted to the occurrence of "minor" spalling in the HSC beam. Due to lower porosity of HSC the thermal conductivity of HSC is higher, resulting increase in temperatures of the rebar and concrete in the HSC beam. There was some surface spalling also in the case of the HSC beam in the "intermediate stage" of exposure to fire. The faster rise in temperature is also due to this loss of concrete. This change in concrete temperature almost vanishes at larger depths and can be described by the big distance from the exposed surface comparatively which decreases the effect of density and spalling on the distribution of temperature in the HSC beam. Figure 3.9 shows the changes of temperatures of rebar and concrete as a function of exposure time to fire for NSC beam B-2 and HSC beam B-4 exposed to SF. The temperature of fire rises quickly in the first ten minutes, then maintains up to about 60 minutes, before a decay curve in the cooling phase. The temperatures of rebar and concrete in the NSC beam are a little more than those of the HSC beam mainly in the heating phase of the fire exposure time. This is contrary to what was noticed for beams B-l and B-3 (exposed to ASTM El 19-standard fire).

4.5 Structural behaviour

4.5.1.1 Deflection

The output mid-span deflection for beams is shown in Figure 4.11 as a function of exposure time to fire. The mid-span deflection of all the six beams increases gradually with time at the early stages of exposure to fire because of thermal expansion and the reduction of stiffness and strength properties of reinforcing steel and concrete with increased temperature. The early deformation of the beam results primarily from thermal gradients developed within the cross-section of beam and the loading applied. Though, the creep effect becomes obvious in the later

phases of fire exposure due to increased temperatures in steel and concrete, and due to substantial deterioration in the stiffness of the beam. This is one of the key reasons for the rise in the deformations in beams B-l, B-3 and B-5 towards the later stages of exposure to fire. Before failure these beams experienced very much elevated temperatures (in steel and concrete) resulting in high stress levels which yield high creep deformations. However, beams B-2, B-4 and B-6 did not attain such high temperatures due to the cooling phase and thus substantial creep deformation might not have arisen in these beams.

The concrete strength effect on the response of fire of RC beams can be showed by comparing the deflection-time curves of beams B-l and B-3 (subjected to the ASTM El 19 fire) in Figure 3.11. The mid-span deflection in beam B-3 (HSC beam) is higher than that of beam B-l (NSC beam) during the entire standard fire exposure. The higher deflection in beam B-3 (HSC beam) resulted from the higher temperature of rebar in that beam and also the quicker degradation of stiffness and strength of the HSC. The larger deflection led to early failure of HSC beam (B3) resulting in lower fire resistance. The failure of the HSC beam seemed to be brittle to that of the NSC beam comparatively.

Structural behaviour of RC beams in fire can be evaluated by studying the deflection trends in Figure 4.11. The deflection of the two beams (B-l and B-3) exposed to the ASTM El 19 standard fire rises throughout the fire exposure time. However, the figure displays recovery in the mid-span deflection for the beams exposed to the design fire scenarios except for beam B5. This can be due to the recovery in the stiffness and strength once the beam enters the cooling phase. Because of the high loading levels and the longer duration of the 'growth phase' of the fire, beam B-5 failed before the temperature of rebar entered the cooling phase. Thus, no deflection recovery was observed for B-5.

4.5.1.2 Axial restraint force

The axial restraint force measured for the two tested axially restrained beams (HSC beam B-6 and NSC beam B-2) is presented in Figure 3.12 as a function of fire exposure time. In the first 100 minutes, the axial force in both beams increased with fire exposure time. This can be due to restraining the thermal expansion of the beam which increased with fire exposure time due to the increase in rebar and concrete temperatures. The rate of increase in the axial restraint force is lower in beam B6 as compared to beam B2. This can be mainly attributed to the severe spalling that occurred at the early stages of fire exposure in HSC beam B6 which reduced the axial stiffness and resulted in the development of smaller axial restraint forces, see Figure 4.12.

Figure 3.12 also shows that after 100 minutes; the axial force was almost constant in beam B2 for about 40 minutes. This was followed by a gradual decrease in the axial restraint force. The plateau in the axial restraint force between 100 minutes and 140 minutes (in beam B2) can be attributed to the relief valve in the restraint system which reduces the axial restraint stiffness to zero.

However, for beam B6, a reduction in the axial restraint force occurred between 100 and 140 minutes of fire exposure. This is due to the severe long design fire, to which this beam was exposed. In B6 the faster degradation of strength and stiffness of HSC contributed to the reduction in the axial force.

The results presented in Figure 3.12 show that HSC beams may develop smaller axial restraint forces under fire conditions when compared with NSC beams. This can be primarily attributed to the fact that HSC is more prone to the quicker decrease in strength as well as stiffness in HSC, as compared to NSC. It can also be attributed to the differences in the thermal strain of HSC from that of NSC. This result suggests that HSC might have a lower thermal strain than that of NSC.

4.6 Summary

Details of model of fire resistance tests on six RC beams were discussed in this chapter. The test parameters discussed were support conditions, concrete strength, fire scenario, and load ratio. Results from fire tests was utilized to describe the comparative performance of NSC and HSC beams exposed to different fire, restraint and loading variations. Results from the tests showed that NSC beams are more fire resistant than HSC beams. The type of fire scenario, axial restraint, and load level were found to influence the overall fire resistance of RC beams. Results from the fire tests provide a better comprehension of the response of RC beams exposed to realistic fire, load, and restraint conditions.

FIGURES OF CHAPTER 4

Table 4-1 Beams

Beam	Concrete Type	Fire Exposure	Support Conditions	P (kN)
B1	NSC	ASTM E119	SS	50
B2	NSC	SF	SS	50
B3	HSC	ASTM E119	SS	50
B4	HSC	SF	SS	50
B5	HSC	LF	SS	50

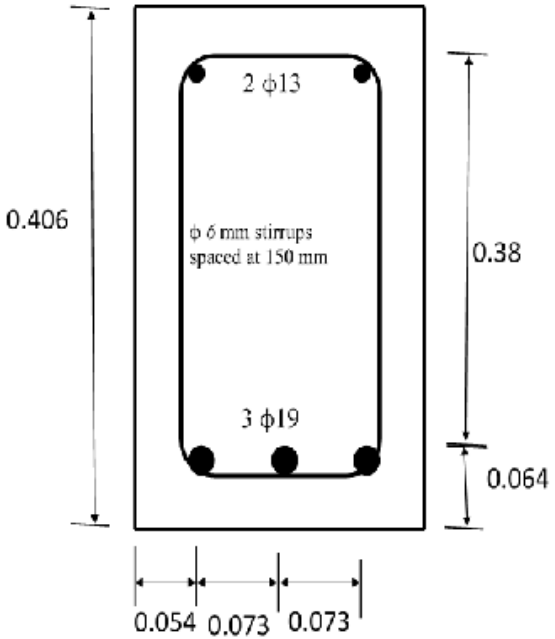

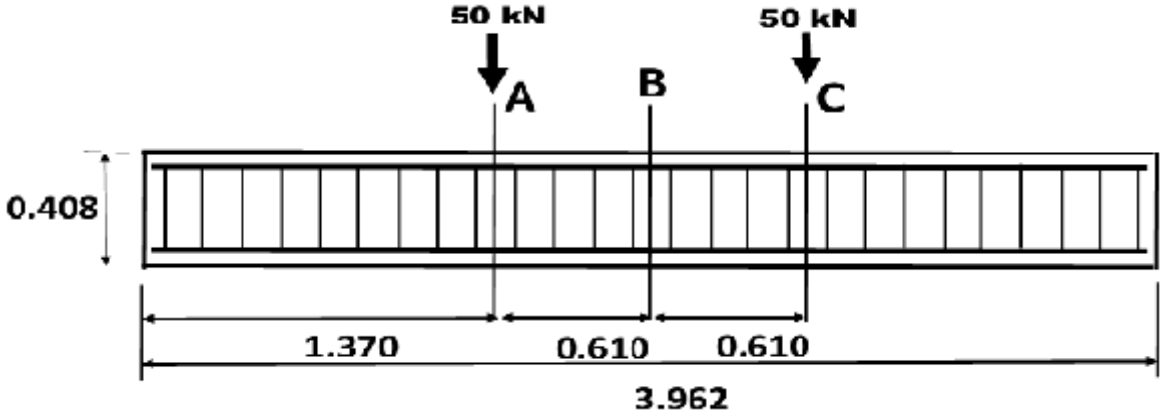

All units in mm.

CHAPTER 5

CONCLUSIONS AND RECOMMENDATIONS

5.1 General

The structural response of HSC beams under fire exposures was investigated in this study. A code was introduced to trace the structural response of HSC beams exposed to realistic fire, loading and restraint joints. All the critical factors, namely, high temperature material properties, different strain components, and the fire induced restraint effect that have significant influence on the fire response of SCC beams are incorporated in the model. First the new material SCC was developed in materials library of OpenSees. For validating the new material properties few codes were written using newly introduced material and compared with the results provided by the official website of OpenSees. Than using the new material in OpenSees, six RC beams were anlyzed under varying fire, concrete strength, load level, and restraint conditions.

5.2 Key observations

On the base of study presented in the thesis, the following are the key findings:

• There is very limited information on the fire performance of RC beams, especially under design fires and realistic loading scenarios

• Fire resistance analysis using OpenSees on RC beams provide unique data on the behavior of NSC and HSC beams under realistic fire load.

• The fire resistance of HSC beams is lower than that of NSC beams with brittle failure occurring in HSC beams.

5.3 Recommendations for future research

While this study has advanced the state-of-the-art with respect to fire response of RC/ SCC beams, further research is required to fully characterize the complex behavior of concrete members under fire exposure. The following are some of the key recommendations for further research in this area:

• Experimental validation may be carried out in subsequent works

Software Expert may be involved in further improvements in OpenSees software in temperature modelling

More investigation is needed to study the effect of occurrence of spalling of high strength concrete beams and capture its effects in software

REFERENCES

APPENDICES

APPENDIX A

MATERIAL PROPERTIES AT ELEVATED TEMPERATURES

This Appendix provides a summary of high temperatures material property relationships used in the numerical model and parametric studies. Information is presented for concrete, steel, FRP, and insulation, with respect to both thermal (specific heat, thermal conductivity) and mechanical (strength, stiffness) properties.

A.1 Concrete – ASCE properties

These equations presented in this section have been reproduced after Lie (1992).

A.1.1 Thermal Capacity, $\rho_{c,T} c_{c,T}$

For siliceous aggregate concrete, with T_c in °C and $\rho_{c,T} C_{c,T}$ *in J / m*

$$0 \le T_c \le 200: \quad \rho_{c,T} c_{c,T} = (0.005 T_c + 1.7) \times 10^6$$

$$200 \le T_c \le 400: \quad \rho_{c,T} c_{c,T} = 2.7 \times 10^6$$

$$400 \le T_c \le 500: \quad \rho_{c,T} c_{c,T} = (0.013 T_c - 2.5) \times 10^6$$

$$500 \le T_c \le 600: \quad \rho_{c,T} c_{c,T} = (-0.013 T_c + 10.5) \times 10^6$$

$$T_c \ge 3316: \quad \rho_{c,T} c_{c,T} = 2.7 \times 10^6$$

For carbonate aggregate concrete

$$0 \le T_c \le 400: \qquad \rho_{c,T} c_{c,T} = 2.566 \times 10^6$$

$$400 \le T_c \le 410: \qquad \rho_{c,T} c_{c,T} = (0.1765T - 68.034) \times 10^6$$

$$410 \le T_c \le 445: \qquad \rho_{c,T} c_{c,T} = (-0.05043T + 25.00671) \times 10^6$$

$$445 \le T_c \le 500: \qquad \rho_{c,T} c_{c,T} = 2.566 \times 10^6$$

$$500 \le T_c \le 635: \qquad \rho_{c,T} c_{c,T} = (0.01603T - 5.44881) \times 10^6$$

$$635 \le T_c \le 715: \qquad \rho_{c,T} c_{c,T} = (0.005T - 100.90225) \times 10^6$$

$$715 \le T_c \le 785: \qquad \rho_{c,T} c_{c,T} = (-0.22103T + 176.07343) \times 10^6$$

$$T_c \ge 785: \qquad \rho_{c,T} c_{c,T} = 2.566 \times 10^6$$

For lightweight aggregate concrete

$$0 \le T_c \le 400: \qquad \rho_{c,T} c_{c,T} = 1.930 \times 10^6$$

$$400 \le T_c \le 420: \qquad \rho_{c,T} c_{c,T} = (0.0772T - 28.95) \times 10^6$$

$$420 \le T_c \le 435: \qquad \rho_{c,T} c_{c,T} = (-0.1029T + 46.706) \times 10^6$$

$$435 \le T_c \le 600: \qquad \rho_{c,T} c_{c,T} = 1.930 \times 10^6$$

$$600 \le T_c \le 700: \qquad \rho_{c,T} c_{c,T} = (0.03474T - 18.9140) \times 10^6$$

$$700 \le T_c \le 720: \qquad \rho_{c,T} c_{c,T} = (-0.1737T + 126.994) \times 10^6$$

$$T_c \le 720: \qquad \rho_{c,T} c_{c,T} = 1.930 \times 10^6$$

A.1.2 Thermal Conductivity, $k_{c,T}$

For siliceous aggregate concrete, with T_c in $°C$ and $k_{c,T}$ in $W/m°C$

$0 \le T_c \le 800:$ $\quad k_{c,T} = -0.000625T_c + 1.5$

$T_c \ge 800:$ $\quad k_{c,T} = 1.0$

For carbonate aggregate concrete

$0 \le T_c \le 293:$ $\quad k_{c,T} = 1.355$

$T_c \ge 293:$ $\quad k_{c,T} = -0.001241T_c + 1.7162$

For lightweight aggregate concrete

$0 \le T_c \le 600:$ $\quad k_{c,T} = -0.00039583T_c + 0.925$

$T_c \ge 600:$ $\quad k_{c,T} = 0.6875$

A.1.3 Thermal Strain (All Type)

$$\varepsilon_{th} = \left[0.004\left(T^2 - 400\right) + 6\left(T - 20\right)\right] \times 10^{-6}$$

A.1.4 Stress-Strain Relationships

$$\sigma_c = \begin{Bmatrix} f'_{c,T}\left[1 - \left(\dfrac{\varepsilon - \varepsilon_{\max,T}}{\varepsilon_{\max,T}}\right)^2\right], & \varepsilon \le \varepsilon_{\max,T} \\ f'_{c,T}\left[1 - \left(\dfrac{\varepsilon_{\max,T} - \varepsilon}{3\varepsilon_{\max,T}}\right)^2\right], & \varepsilon > \varepsilon_{\max,T} \end{Bmatrix}$$

$$f'_{c,T} = \begin{Bmatrix} f'_c & ,20°C \le T \le 450°C \\ f'_c\left[2.011 - 2.353\left(\frac{T-20}{1000}\right)\right] & ,450°C < T \le 874°C \\ 0 & ,874°C < T \end{Bmatrix}$$

$$\varepsilon_{\max,T} = 0.0025 + \left(6.0T + 0.04T^2\right) \times 10^{-6}$$

A.2 Concrete – Eurocode properties

These equations presented in this section have been reproduced after Eurocode 2 (2004)

A.2.1 Thermal Capacity

Specific Heat (J/kg-°C)

$c = 900$ *for* $20°C \le T \le 100°C$

$c = 900 + (T - 100)$ *for* $100°C < T \le 200°C$

$c = 1000 + (T - 200)/2$ *for* $200°C < T \le 400°C$

$c = 1100$ *for* $400°C < T \le 1200°C$

Density (kg/m^3)

$\rho = \rho(20°C)$ *for* $20°C \le T \le 115°C$

$\rho = \rho(20°C)\ (1 - 0.02(T - 115)/85)$ *for* $115°C < T \le 200°C$

$\rho = \rho(20°C)\ (0.98 - 0.03(T - 200)/200)$ *for* $200°C < T \le 400°C$

$\rho = \rho(20°C)\ (0.95 - 0.07(T - 400)/800)$ *for* $400°C < T \le 1200°C$

*A.2.2 Thermal Conductivity (*All Type*)*

Upper Limit

$k_c = 2 - 0.2451\ (T / 100) + 0.0107\ (T / 100)2$ *for* $20°C \le T \le 1200°C$

Lower Limit

$$k_c = 1.36 - 0.136\,(T / 100) + 0.0057\,(T / 100)2 \quad for\ 20°C \le T \le 1200°C$$

A.2.3 Thermal Strain

Siliceous Aggregate

$$\varepsilon_{th} = -1.8\times10^{-4} + 9\times10^{-6}T + 2.3 \times 10^{-11}T^3 \quad for\ 20°C \le T \le 700°C$$

$$\varepsilon_{th} = 14 \times 10^{-3} \quad for\ 700°C < T \le 1200°C$$

Carbonate Aggregate

$$\varepsilon_{th} = -1.2\times10^{-4} + 6\times10^{-6}T + 1.4\times10^{-11}T^3 \quad for\ 20°C \le T \le 805°C$$

$$\varepsilon_{th} = 12 \times 10^{-3} \quad for\ 805°C < T \le 1200°C$$

A.2.4 Stress-Strain Relationship

$$\sigma_c = \frac{3\varepsilon\, f'_{c,T}}{\varepsilon_{c1,T}\left(2 + \left(\frac{\varepsilon}{\varepsilon_{c1,T}}\right)^3\right)} \quad , \varepsilon \le \varepsilon_{cu1,T}$$

For $\varepsilon_{c1(T)} < \varepsilon \le \varepsilon_{cu1(T)}$, the Eurocode permits the use of linear as well as nonlinear descending branch in the numerical analysis. For the parameters in this equation refer to Table A.1.

Table A.1 Values for the Main Parameters of the Stress-strain Relationships of NSC at Elevated Temperatures (Eurocode 2)

T(°C)	Normal Strength Concrete					
	Siliceous Aggregate			Calcareous Aggregate		
	$\frac{f_{c,T}^{'}}{f_{c}^{'}(20^{\circ}C)}$	$\varepsilon_{c1,T}$	$\varepsilon_{cu1,T}$	$\frac{f_{c,T}^{'}}{f_{c}^{'}(20^{\circ}C)}$	$\varepsilon_{c1,T}$	$\varepsilon_{cu1,T}$
20	1	0.0025	0.02	1	0.0025	0.02
100	1	0.004	0.0225	1	0.004	0.023
200	0.95	0.0055	0.025	0.97	0.0055	0.025
300	0.85	0.007	0.0275	0.91	0.007	0.028
400	0.75	0.01	0.03	0.85	0.01	0.03
500	0.6	0.015	0.0325	0.74	0.015	0.033
600	0.45	0.025	0.035	0.6	0.025	0.035
700	0.3	0.025	0.0375	0.43	0.025	0.038
800	0.15	0.025	0.04	0.27	0.025	0.04
900	0.08	0.025	0.0425	0.15	0.025	0.043
1000	0.04	0.025	0.045	0.06	0.025	0.045
1100	0.01	0.025	0.0475	0.02	0.025	0.048
1200	0	-	-	0	-	-

A.3 Reinforcing steel – ASCE properties

A.3.1 Thermal Strain

$$\varepsilon_{ths} = \left[0.004\left(T^2 - 400\right) + 6\left(T - 20\right)\right] \times 10^{-6} \qquad T < 1000°C$$

A.3.2 Stress-strain Relationship

$$\sigma_s = \begin{cases} \dfrac{f\left(T, 0.001\right)}{0.001}\varepsilon_s & \varepsilon_s \le \varepsilon_p \\ \dfrac{f\left(T, 0.001\right)}{0.001}\varepsilon_p + f\left(T, \varepsilon_s - \varepsilon_p + 0.001\right) - f\left(T, 0.001\right) & \varepsilon_s > \varepsilon_p \end{cases}$$

$$f\left(T, x\right) = 6.9\left(50 - 0.04T\right)\left[1 - \exp\left(\left(-30 + 0.03T\right)\sqrt{x}\right)\right]$$

$$\varepsilon_p = 4 \times 10^{-6} f_{y,20}$$

where: σ_s and ε_s = stress (MPa) and strain in steel reinforcement, respectively, and $f_{y,20}$ is the yield strength of reinforcing steel (MPa) at room temperature.

A.4 Reinforcing steel – Eurocode properties

A.4.1 Thermal Strain

$$\varepsilon_{ths} = \begin{cases} 1.2 \times 10^{-5} T + 0.4 \times 10^{-8} T^2 - 2.416 \times 10^{-4} & 20°C \le T < 750°C \\ 1.1 \times 10^{-2} & 750°C \le T < 860°C \\ 2 \times 10^{-5} T - 6.2 \times 10^{-3} & 20°C \le T < 750°C \end{cases}$$

A.4.2 Stress-strain Relationship

$$\sigma_s = \begin{cases} \varepsilon_s E_{s,T} & \varepsilon_s \le \varepsilon_{sp,T} \\ f_{sp,T} - c + (b/a)\left(a^2 - \left(\varepsilon_{sy,T} - \varepsilon_s \right)^2 \right)^{0.5} & \varepsilon_{sp,T} < \varepsilon_s \le \varepsilon_{sy,T} \\ f_{sy,T} & \varepsilon_{sy,T} < \varepsilon_s \le \varepsilon_{st,T} \\ f_{sy,T}\left(1 - \dfrac{\varepsilon_s - \varepsilon_{st,T}}{\varepsilon_{su,T} - \varepsilon_{st,T}} \right) & \varepsilon_{st,T} < \varepsilon_s \le \varepsilon_{su,T} \\ 0.0 & \varepsilon_s > \varepsilon_{su,T} \end{cases}$$

Parameters

$$\varepsilon_{sp,T} = \frac{f_{sp,T}}{E_{s,T}} \qquad \varepsilon_{sy,T} = 0.02 \qquad \varepsilon_{st,T} = 0.15 \qquad \varepsilon_{su,T} = 0.2$$

Functions

$$a^2 = \left(\varepsilon_{sy,T} - \varepsilon_{sp,T} \right)\left(\varepsilon_{sy,T} - \varepsilon_{sp,T} + \frac{c}{E_{s,T}} \right)$$

$$b^2 = c\left(\varepsilon_{sy,T} - \varepsilon_{sp,T} \right) E_{s,T} + c^2$$

$$c = \frac{\left(f_{sy,T} - f_{sp,T} \right)^2}{\left(\varepsilon_{sy,T} - \varepsilon_{sp,T} \right) E_{s,T} - \left(f_{sy,T} - f_{sp,T} \right)}$$

The values of $f_{sp,T}$, $f_{sy,T}$ and $E_{s,T}$ can be obtained from Table A.2

Table A.2 Values for the Main Parameters of the Stress-strain Relationships of Reinforcing Steel at Elevated Temperatures (Eurocode 2)

Steel Temperature T (°C)	f_{yT} / f_y	f_{sp} / f_y *	E_{sT} / E_s *
20	1	1	1
100	1	1	1
200	1	0.807	0.9
300	1	0.613	0.8
400	1	0.42	0.7
500	0.78	0.36	0.6
600	0.47	0.18	0.31
700	0.23	0.075	0.13
800	0.11	0.05	0.09
900	0.06	0.0375	0.0675
1000	0.04	0.025	0.045
1100	0.02	0.0125	0.0225
1200	0	0	0

* f_y and E_s are yield strength and modulus of elasticity at room temperature

APPENDIX B

COMPUTER CODES

B.1 Uniaxial material at elevated temperature

B.1.1 Steel01Thermal

```
double Steel01Thermal::setThermalTangentAndElongation(double &TempT,
double&ET, double&Elong)
{// EN 1993 pt 1-2-1.
if (TempT <= 100) {
fy = fyT;
E0 = E0T;
}
else if (TempT <= 200) {
fy = fyT;
E0 = E0T*(1 - (TempT - 100)*0.1/100);
}
else if (TempT <= 300) {
fy = fyT;
E0 = E0T*(0.9 - (TempT - 200)*0.1/100);
}
else if (TempT <= 400) {
fy = fyT;
E0 = E0T*(0.8 - (TempT - 300)*0.1/100);
}
else if (TempT <= 500) {
fy = fyT*(1 - (TempT - 400)*0.22/100);
E0 = E0T*(0.7 - (TempT - 400)*0.1/100);
}
else if (TempT <= 600) {
fy = fyT*(0.78 - (TempT - 500)*0.31/100);
E0 = E0T*(0.6 - (TempT - 500)*0.29/100);
}
else if (TempT <= 700) {
fy = fyT*(0.47 - (TempT - 600)*0.24/100);
E0 = E0T*(0.31 - (TempT - 600)*0.18/100);
}
else if (TempT <= 800) {
```



```
fy = fyT*(0.23 - (TempT - 700)*0.12/100);
E0 = E0T*(0.13 - (TempT - 700)*0.04/100);
}
else if (TempT <= 900) {
fy = fyT*(0.11 - (TempT - 800)*0.05/100);
E0 = E0T*(0.09 - (TempT - 800)*0.02/100);
}
else if (TempT <= 1000) {
fy = fyT*(0.06 - (TempT - 900)*0.02/100);
E0 = E0T*(0.0675 - (TempT - 900)*(0.00675 - 0.0045)/100);
}
```

```
else if (TempT <= 1100) {
fy = fyT*(0.04 - (TempT - 1000)*0.02/100);
E0 = E0T*(0.045 - (TempT - 1000)*(0.0045 - 0.00225)/100);
}
else if (TempT <= 1200) {
fy = fyT*(0.02 - (TempT - 1100)*0.02/100);
E0 = E0T*(0.0225 - (TempT - 1100)*0.0225/100);
}
else {
opserr << "the temperature is invalid\n";
}
// caculation of thermal elongation of reinforcing steel. JZ
else if (TempT <= 750) {
ThermalElongation = -2.416e-4 + 1.2e-5 *(TempT) + 0.4e-8
*(TempT)^2);
}
else if (TempT <= 1200) {
ThermalElongation = 11e-3;
}
else if (TempT <= 1180) {
ThermalElongation = -6.2e-3 + 2e-5*TempT;
}
else {
opserr << "the temperature is invalid\n";
}
ET = E0;
Elong = ThermalElongation;
return 0;}
```

228

Figure A.1: Function "Steel01Thermal::setThermalTangentAndElongation ()"

B.1.2 Concrete02Thermal

```
double Concrete02Thermal::setThermalTangentAndElongation(double &TempT,
double&ET, double&Elong)
{//material properties with temperature
// Temp (TempT) is actural temperature; ambient temperature is 20;
// Siliceous aggregates
// The datas are from EN 1992 part 1-2-1
// Tensile strength at elevated temperature
if (TempT <= 100) {
ft = ft0;
Ets = Ets0;
}
else if (TempT <= 600) {
ft = ft0*(1.0 - 1.0*(TempT -100)/500);
Ets = Ets0*(1.0 - 1.0*(TempT -100)/500);
}
else {
ft = 0;
Ets = 0;
```

```
}
// Compression strength, at elevated TempTerature, Siliceous
aggregates
// Maximum temperature is 1100
// Strain at compression strength, at elevated temperature
// Ultimate (crushing) strain, at elevated temperature
if (TempT <= 20) {
fc = fc0;
epsc0 = -0.0025;
fcu = fcu0;
epscu = -0.02;
}
else if (TempT <= 100) {
fc = fc0;
epsc0 = -(0.0025 + (0.004-0.0025)*(TempT - 20)/80);
fcu = fcu0;
epscu = -(0.0200 + (0.0225-0.0200)*(TempT - 20)/80);
}
else if (TempT <= 200) {
fc = fc0*(1 - (TempT - 100)*0.05/100);
epsc0 = -(0.0040 + (0.0055-0.0040)*(TempT - 100)/100);
fcu = fcu0*(1 - (Temp - 100)*0.05/100);
epscu = -(0.0225 + 0.0025*(Temp - 100)/100);
}
else if (TempT <= 300) {
```



```
fc = fc0*(0.95 - (TempT - 200)*0.1/100);
epsc0 = -(0.0055 + (0.0070-0.0055)*(TempT - 200)/100);
fcu = fcu0*(0.95 - (TempT - 200)*0.1/100);
epscu = -(0.0250 + 0.0025*(TempT - 200)/100);
}
else if (TempT <= 400) {
fc = fc0*(0.85 - (TempT - 300)*0.1/100);
epsc0 = -(0.0070 + (0.0100-0.0070)*(TempT - 300)/100);
fcu = fcu0*(0.85 - (TempT - 300)*0.1/100);
epscu = -(0.0275 + 0.0025*(TempT - 300)/100);
}
else if (TempT <= 500) {
fc = fc0*(0.75 - (TempT - 400)*0.15/100);
epsc0 = -(0.0100 + (0.0150-0.0100)*(TempT - 400)/100);
fcu = fcu0*(0.75 - (TempT - 400)*0.15/100);
epscu = -(0.03 + 0.0025*(TempT - 400)/100);
}
else if (TempT <= 600) {
fc = fc0*(0.60 - (TempT - 500)*0.15/100);
epsc0 = -(0.0150 + (0.0250-0.0150)*(TempT - 500)/100);
fcu = fcu0*(0.60 - (TempT - 500)*0.15/100);
epscu = -(0.0325 + 0.0025*(TempT - 500)/100);
}
else if (TempT <= 700) {
fc = fc0*(0.45 - (TempT - 600)*0.15/100);
epsc0 = -0.0250;
```

```
fcu = fcu0*(0.45  - (TempT  - 600)*0.15/100);
epscu = -(0.035  + 0.0025*(TempT  - 600)/100);
}
else if (TempT <= 800) {
fc = fc0*(0.30  - (TempT  - 700)*0.15/100);
epsc0 = -0.0250;
fcu = fcu0*(0.30  - (TempT  - 700)*0.15/100);
epscu = -(0.0375  + 0.0025*(TempT  - 700)/100);
}
else if (TempT <= 900) {
fc = fc0*(0.15  - (TempT  - 800)*0.07/100);
epsc0 = -0.0250;
fcu = fcu0*(0.15  - (TempT  - 800)*0.07/100);
epscu = -(0.04  + 0.0025*(TempT  - 800)/100);
}
else if (TempT <= 1000) {
fc = fc0*(0.08  - (TempT  - 900)*0.04/100);
epsc0 = -0.0250;
fcu = fcu0*(0.08  - (TempT  - 900)*0.04/100);
epscu = -(0.0425  + 0.0025*(TempT  - 900)/100);
}
else if (TempT <= 1100) {
fc = fc0*(0.04  - (TempT  - 1000)*0.03/100);
epsc0 = -0.0250;
fcu = fcu0*(0.04  - (TempT  - 1000)*0.03/100);
epscu = -(0.045  + 0.0025*(TempT  - 1000)/100);
}
else {
opserr << "the temperature is invalid\n";
}
230
// calculation of thermal elongation, Siliceous aggregates
if (TempT  <= 20) {
ThermalElongation  = 0.0;
}
else if (TempT <= 700) {
ThermalElongation  = -1.8e-4  + 9e-6 *TempT + 2.3e-11  *TempT^3
}
else if (TempT <= 1200) {
ThermalElongation  = 14e-3;
}
else {
opserr << "the temperature is invalid\n";
}
```

B.2 FiberSection2dThermal

```
const Vector&
FiberSection2dThermal::getTemperatureStress(double *dataMixed)
{
double yBarT = 0;
sTData[0] = 0.0; sTData[1] = 0.0;
double fiberLocs[10000];
double fiberArea[10000];
if (sectionIntegr != 0) {
sectionIntegr->getFiberLocations(numFibers, fiberLocs);
sectionIntegr->getFiberWeights(numFibers, fiberArea);
}
else {
for (int i = 0; i < numFibers; i++) {
fiberLocs[i] = matData[2*i];
fiberArea[i] = matData[2*i+1];
}
}
double dataTempe[18];
for (int i = 0; i < 18; i++) {
dataTempe[i] = dataMixed[i];
}
//JJadd, 12/2010, updata yBar = Ai*Ei*yi/(Ai*E*) start
double ThermalTangent[100];
double ThermalElongation[100];
for (int i = 0; i < numFibers; i++) {
ThermalTangent[i]=0;
ThermalElongation[i]=0;
}
for (int i = 0; i < numFibers; i++) {
UniaxialMaterial *theMat = theMaterials[i];
double yi = fiberLocs[i];
double Ai = fiberArea[i];
239
double FiberTemperature = 0 ; //JZ
//if locY1 and locY9 are not less than zero
if ( fabs(dataTempe[1]) <= 1e-10 && fabs(dataTempe[17]) <= 1e-
10 ) //no tempe load
{
FiberTemperature = 0;
}
else
{
//caculate the fiber tempe, T=T1-(Y-Y1)*(T1-T2)/(Y1-Y2)
if ( fiberLocs[i] <= dataTempe[1])
{
opserr
<<"FiberSection2dThermal::setTrialSectionDeformationTemperature --
```

```
fiber loc is out of the section";
}
else if (fiberLocs[i] <= dataTempe[3])
{
FiberTemperature  = dataTempe[0]  - (dataTempe[1]  - fiberLocs[i])  *
(dataTempe[0]  - dataTempe[2])/(dataTempe[1]  - dataTempe[3]);
}
else if ( fiberLocs[i] <= dataTempe[5] )
{
FiberTemperature  = dataTempe[2]  - (dataTempe[3]  - fiberLocs[i])  *
(dataTempe[2]  - dataTempe[4])/(dataTempe[3]  - dataTempe[5]);
}
else if ( fiberLocs[i] <= dataTempe[7] )
{
FiberTemperature  = dataTempe[4]  - (dataTempe[5]  - fiberLocs[i])  *
(dataTempe[4]  - dataTempe[6])/(dataTempe[5]  - dataTempe[7]);
}
else if ( fiberLocs[i] <= dataTempe[9] )
{
FiberTemperature  = dataTempe[6]  - (dataTempe[7]  - fiberLocs[i])  *
(dataTempe[6]  - dataTempe[8])/(dataTempe[7]  - dataTempe[9]);
}
else if (fiberLocs[i] <= dataTempe[11] )
{
240
FiberTemperature  = dataTempe[8]  - (dataTempe[9]  - fiberLocs[i])  *
(dataTempe[8]  - dataTempe[10])/(dataTempe[9]  - dataTempe[11]);
}
else if (fiberLocs[i] <= dataTempe[13] )
{
FiberTemperature  = dataTempe[10]  - (dataTempe[11]  - fiberLocs[i])  *
(dataTempe[10]  - dataTempe[12])/(dataTempe[11]  - dataTempe[13]);
}
else if (fiberLocs[i] <= dataTempe[15] )
{
FiberTemperature  = dataTempe[12]  - (dataTempe[13]  - fiberLocs[i])  *
(dataTempe[12]  - dataTempe[14])/(dataTempe[13]  - dataTempe[15]);
}
else if ( fiberLocs[i] <= dataTempe[17] )
{
FiberTemperature  = dataTempe[14]  - (dataTempe[15]  - fiberLocs[i])  *
(dataTempe[14]  - dataTempe[16])/(dataTempe[15]  - dataTempe[17]);
}
else
{
opserr
<<"FiberSection2dThermal::setTrialSectionDeformationTemperature  --
fiber loc is out of the section";
}
}
// determine material strain and set it
double tangent, elongation;
```

```
theMat->setThermalTangentAndElongation(FiberTemperature, tangent,
elongation);
ThermalTangent[i]=tangent;
ThermalElongation[i]=elongation;
}
//calculate centroid of section yBar for composite section,i.e. yBar
is related to tangent E
double SigmaEAy  = 0;
double SigmaEA  = 0;
for (int i = 0; i < numFibers; i++) {
241
SigmaEAy  += ThermalTangent[i]*fiberArea[i]*fiberLocs[i];
SigmaEA  += ThermalTangent[i]*fiberArea[i];
}
yBarT = SigmaEAy/SigmaEA;
// calculate section resisting force due to thermal load
double FiberForce;
for (int i = 0; i < numFibers; i++) {
FiberForce  = ThermalTangent[i]*fiberArea[i]*ThermalElongation[i];
sTData[0] += FiberForce;
sTData[1] -= FiberForce*(fiberLocs[i]  - yBarT);
}
return *sT;
}
```

Figure B.1: Function of "FiberSection2dThermal::getTemperatureStress()"

242

B.3 DispBeamColumn2dThermal

```
DispBeamColumn2dThermal::addLoad(ElementalLoad  *theLoad, double
loadFactor)
{
int type;
const Vector &data = theLoad->getData(type, loadFactor);
double L = crdTransf->getInitialLength();
if (type == LOAD_TAG_Beam2dUniformLoad)  {…}
else if (type == LOAD_TAG_Beam2dPointLoad){…}
else if (type == LOAD_TAG_Beam2dThermalAction)  {
dataMix = data*loadFactor;
counterTemperature = 0;
q0Temperature[0]  = 0.0;
q0Temperature[1]  = 0.0;
q0Temperature[2]  = 0.0;
//const Matrix &pts = quadRule.getIntegrPointCoords(numSections);
//const Vector &wts = quadRule.getIntegrPointWeights(numSections);
double xi[maxNumSections];
```

```
beamInt->getSectionLocations(numSections, L, xi);
double wt[maxNumSections];
beamInt->getSectionWeights(numSections, L, wt);
// Loop over the integration points
for (int i = 0; i < numSections; i++) {
int order = theSections[i]->getOrder();
const ID &code = theSections[i]->getType();
//double xi6 = 6.0*pts(i,0);
double xi6 = 6.0*xi[i];
// Get section stress resultant
const Vector &s = theSections[i]->getTemperatureStress(dataMix);
// Perform numerical integration on internal force
//q.addMatrixTransposeVector(1.0, *B, s, wts(i));
double si;
for (int j = 0; j < order; j++) {
//si = s(j)*wts(i);
si = s(j)*wt[i];
```

243

```
switch(code(j)) {
case SECTION_RESPONSE_P:
q0Temperature[0] += si; break;
case SECTION_RESPONSE_MZ:
q0Temperature[1] += (xi6-4.0)*si; q0Temperature[2] += (xi6-
2.0)*si; break;
default:
break;
}}} }
return 0;
}
```

Figure C.1: Function of "DisBeamColumn2dThermal::addLoad()"

```
const Vector&
DispBeamColumn2dTemperature::getResistingForce()
{
double xi[maxNumSections];
beamInt->getSectionLocations(numSections, L, xi);
double wt[maxNumSections];
beamInt->getSectionWeights(numSections, L, wt);
// Zero for integration
q.Zero();
this->update();// added to update stress state before getting
resultant stress to consider material softening.
// Loop over the integration points
for (int i = 0; i < numSections; i++) {
int order = theSections[i]->getOrder();
const ID &code = theSections[i]->getType();
//double xi6 = 6.0*pts(i,0);
double xi6 = 6.0*xi[i];
// Get section stress resultant
const Vector &s = theSections[i]->getStressResultant();
```

```
// Perform numerical integration on internal force
244
//q.addMatrixTransposeVector(1.0, *B, s, wts(i));
double si;
for (int j = 0; j < order; j++) {
//si = s(j)*wts(i);
si = s(j)*wt[i];
switch(code(j)) {
case SECTION_RESPONSE_P:
q(0) += si; break;
case SECTION_RESPONSE_MZ:
q(1) += (xi6-4.0)*si; q(2) += (xi6-2.0)*si; break;
default:
break;
}} }
if (counterTemperature == 0) { //first iteration add thermal
load and no thermal load from second iteration because after this if,
counterTemperature++.
//thermal force = EA*alpha*DeltaT= EA*alpha*(Ti-Ti-1)
q(0) -= (q0Temperature[0] - q0TemperatureP[0]);
q(1) -= (q0Temperature[1] - q0TemperatureP[1]);
q(2) -= (q0Temperature[2] - q0TemperatureP[2]);
q0TemperatureP[0] = q0Temperature[0];
q0TemperatureP[1] = q0Temperature[1];
q0TemperatureP[2] = q0Temperature[2];
}
counterTemperature++;
// Add effects of element loads, q = q(v) + q0
q(0) += q0[0];
q(1) += q0[1];
q(2) += q0[2];
// Vector for reactions in basic system
Vector p0Vec(p0, 3);
P = crdTransf->getGlobalResistingForce(q, p0Vec);
return P;
}
```

Figure C.2: Function of "DisBeamColumn2dThermal::getResistingForce()"

B.4 Scripts of restrained beam

```
# 2D bar element, two elements, subjected to thermal expansion;
# left element thermal expansion, right element ambient temperature
# aimed to use the DispBeamColumn2dThermal to conduct thermal analysis
#--------------------------------------------------------------------------------
# Geometric model
# _________
# left ele1 3 right ele2 | | (2 fibers in section)
# 1 |----------------o--------------|2 |_________ | 0.1m
# |<-------------2m----------->| | |
# |_________|
```

```
# 0.1m
#--------------------------------------------------------------------------------
```

wipe; file mkdir Data;	# create data directory
model BasicBuilder -ndm 2 -ndf 3;	# 2 dimension and 3 dofs per node
source DisplayPlane.tcl;	# procedure for displaying a plane in model
source DisplayModel2D.tcl;	# procedure for displaying 2D perspective of model

```
#define node
node 1 0 0;
node 2 2 0;
node 3 1 0;
#define boundary condition; nodes 1 and 2 are fixed; node 3 translational free.
fix 1 1 1 1;
fix 2 1 1 1;
fix 3 0 1 1;
#define an elastic material with Tag=1 and E=2e11.
uniaxialMaterial ElasticThermal 1 2e11;
#define fibred section; Two fibres: fiber $yLoc $zLoc $A $matTag
set secTag 1;
section FiberThermal $secTag {
fiber -0.025 0 0.005 1;
fiber 0.025 0 0.005 1;
};
#define coordinate transforamtion: geomTransf $type $TransfTag;
#three transformation types can be chosen: Linear, PDelta, Corotational)
246
geomTransf Linear 1 ;
#define element: dispBeamColumnThermal $eleTag $iNode $jNode $numIntgrPts $secTag
$TransfTag;
#"numIntgrPts" is the number of integration points along the element;
#"TransfTag" is pre-defined coordinate-transformation;
element dispBeamColumnThermal 1 1 3 3 1 1;
element dispBeamColumnThermal 2 3 2 3 1 1;
#define output
# displacements of free nodes
recorder Node -file Data/DFree3.out -time -node 3 -dof 1 disp;
recorder Node -file Data/RBase1.out -time -node 1 -dof 1 2 3 reaction; # support reaction
#view the deformation shape
set ViewScale 2;
# display deformed shape, the scaling factor needs to be adjusted for each model
DisplayModel2D DeformedShape $ViewScale ;
#define thermal load (i.e. temperature distribution in section)
#-beamThermal $T1 $LocY1 $T2 LocY2....; two temperature means uniform or linear
temperature distribution
#T1=bottom temperature;T2=top temperature
pattern Plain 2 Linear {
eleLoad -ele 1 -type -beamThermal 1000 -0.05 1000 0.05
eleLoad -ele 2 -type -beamThermal 0 -0.05 0 0.05
};
constraints Plain;
numberer Plain;
system BandGeneral;
```

```
test NormDispIncr 1e-8 10 ;
algorithm Newton;
integrator LoadControl 0.1;
analysis Static;
analyze 10;
loadConst -time 0.0
247
```

B.5 Scripts of beam with finite end restraint

```
# Single steel beam subjected to UDL and thermal gradient
# total 8 elements for 6m beam ;
# distributed load UDL=1000N/m; thermal gradient is linear cross section;
# thermal gradient is define by Tbot and Ttop;
# 8 fibers along the height 0.2m of the beam section;
# Material is temperature-dependent elastic; E=2E11 for ambient temperature(20)
# E is referred to the EN 1993 pt 1-2-1.
# expansion coefficient is constant with value 12e-6
# SI unit i.e. meter, newton
#-----------------------------------------------------------------------------
# Geometric model _____
# | |
# |-------------------------------------|||0.2
# 21&1 2 3 4 5 6 7 8 9&22 |____|
# |<-----------------6m------------------>| 0.1
#
# SET UP ---------------------------------------------------------------------
wipe;
```

model BasicBuilder -ndm 2 -ndf 3;	# 2 dimension and 3 dofs per node
set dataDir Data;	# set up name of data directory (can remove this)
file mkdir $dataDir;	# create data directory

```
source DisplayPlane.tcl
source DisplayModel2D.tcl
```

# nodal coordinates: node 1 0. 0;	node 2 0.75 0.; node 3 1.5 0;	node 4 2.25 0; node 5 3 0;
node 6 3.75 0; node 7 4.5 0;	node 8 5.25 0.; node 9 6 0;	

```
#node 21, 22 for zerolength element to model spring(restraint)
node 21 0 0;
node 22 6. 0.;
# Single point constraints -- Boundary Conditions
fix 1 1 1 0;
248
fix 9 1 1 0;
fix 21 1 1 1;
fix 22 1 1 1;
#define an elastic material with Tag=1 and E=2e11.
set matTag 1;
uniaxialMaterial ElasticThermal $matTag 2e11;
```

```
#define fibred section; define fibre: fiber $yLoc $zLoc $A $matTag
# origin of section is the center of rectangular
set SecTag 1;
section FiberThermal $SecTag {
#8 fibers
fiber 0.0125 0 0.0025 $matTag;
fiber 0.0375 0 0.0025 $matTag;
fiber 0.0625 0 0.0025 $matTag;
fiber 0.0875 0 0.0025 $matTag;
fiber -0.0125 0 0.0025 $matTag;
fiber -0.0375 0 0.0025 $matTag;
fiber -0.0625 0 0.0025 $matTag;
fiber -0.0875 0 0.0025 $matTag;
};
# define geometric transformation: Linear, PDelta, Corotational
set TransfTag 1;
geomTransf Linear $TransfTag;
#geomTransf PDelta $TransfTag;
#geomTransf Corotational $TransfTag;
#define beam element: dispBeamColumnThermal $eleTag $iNode $jNode $numIntgrPts $secTag
$TransfTag;
#"numIntgrPts" is the number of integration points along the element;
#"TransfTag" is pre-defined coordinate-transformation;
set numIntgrPts 3;
element dispBeamColumnThermal 1 1 2 $numIntgrPts $SecTag $TransfTag;
element dispBeamColumnThermal 2 2 3 $numIntgrPts $SecTag $TransfTag;
element dispBeamColumnThermal 3 3 4 $numIntgrPts $SecTag $TransfTag;
249
element dispBeamColumnThermal 4 4 5 $numIntgrPts $SecTag $TransfTag;
element dispBeamColumnThermal 5 5 6 $numIntgrPts $SecTag $TransfTag;
element dispBeamColumnThermal 6 6 7 $numIntgrPts $SecTag $TransfTag;
element dispBeamColumnThermal 7 7 8 $numIntgrPts $SecTag $TransfTag;
element dispBeamColumnThermal 8 8 9 $numIntgrPts $SecTag $TransfTag;
# first define material for zeroLength element;
# elasticity modulus is equal to stiffness of spring
# dir 6 is the rotation around z; dir 1 is the translational dof
uniaxialMaterial Elastic 2 3e6; #translational spring
uniaxialMaterial Elastic 3 6.67e8; # rotational spring
#define element for traslational&rotational spring
element zeroLength 121 1 21 -mat 2 -dir 6; #rotational spring
element zeroLength 922 9 22 -mat 2 -dir 6; #rotational spring
element zeroLength 933 9 22 -mat 3 -dir 1; #translational spring
```

# define output recorder Node -file Data/DFree5.out -time -node 5 -dof 2 disp;	# displacements of free
nodes recorder Node -file Data/DFree9.out -time -node 9 -dof 1 disp; recorder Node -file Data/RBase.out -time -node 1 -dof 1 reaction;	# support reaction

```
recorder Node -file Data/RBase21.out -time -node 21 22 -dof 1 2 3 reaction;
#support reaction
#define load
# first add a UDL
set UDL -1000;
pattern Plain 1 Linear {
```

```
eleLoad -ele 1 -type -beamUniform $UDL 0. 0.;
eleLoad -ele 2 -type -beamUniform $UDL 0. 0.;
eleLoad -ele 3 -type -beamUniform $UDL 0. 0.;
eleLoad -ele 4 -type -beamUniform $UDL 0. 0.;
eleLoad -ele 5 -type -beamUniform $UDL 0. 0.;
eleLoad -ele 6 -type -beamUniform $UDL 0. 0.;
eleLoad -ele 7 -type -beamUniform $UDL 0. 0.;
eleLoad -ele 8 -type -beamUniform $UDL 0. 0.;
250
}
constraints Plain;
numberer Plain;
system BandGeneral;
test NormDispIncr 1e-8 100 ;
algorithm  Newton;
integrator LoadControl 1
analysis Static;
analyze 1;
loadConst -time 0.0
#define thermal load (i.e. temperature distribution  in section)
#-beamThermal $T1 $LocY1 $T2 LocY2....; two temperature means uniform or linear
temperature distribution
# T1 is the bottom temp of beam and T2 is the top
# Y1 is the coordinate of bottom of beam section; Y2 is for top
# the temperature will be interpolated along the section
set T1 1000;set T2 0;
set Y1 -0.1;set Y2 0.1;
pattern Plain 2 Linear {
eleLoad -ele 1 -type -beamThermal $T1 $Y1 $T2 $Y2 ;
eleLoad -ele 2 -type -beamThermal $T1 $Y1 $T2 $Y2 ;
eleLoad -ele 3 -type -beamThermal $T1 $Y1 $T2 $Y2 ;
eleLoad -ele 4 -type -beamThermal $T1 $Y1 $T2 $Y2 ;
eleLoad -ele 5 -type -beamThermal $T1 $Y1 $T2 $Y2 ;
eleLoad -ele 6 -type -beamThermal $T1 $Y1 $T2 $Y2 ;
eleLoad -ele 7 -type -beamThermal $T1 $Y1 $T2 $Y2 ;
eleLoad -ele 8 -type -beamThermal $T1 $Y1 $T2 $Y2 ;
}
integrator LoadControl 0.01
analysis Static;
analyze 100;
loadConst -time 0.0
```

APPENDIX C

ADDITION OF MATERIALS IN OPENSEES MATERIAL LIBRARY

```
// this is the second edition of Concrete02ThermalHSC / SCC,the
interface of it is same with concrete02.
#include <stdlib.h>
#include <Concrete02ThermalSCC.h>
#include <OPS_Globals.h>
#include <float.h>
#include <Channel.h>
#include <Information.h>
#include <elementAPI.h>
#include <OPS_Globals.h>
void *
OPS_NewConcrete02ThermalSCC()
{
  // Pointer to a uniaxial material that will be returned
  UniaxialMaterial *theMaterial = 0;

  int    iData[1];
  double dData[7];
  int numData = 1;

  if (OPS_GetIntInput(&numData, iData) != 0) {
    opserr << "WARNING invalid uniaxialMaterial Concrete02ThermalSCC
tag" << endln;
    return 0;
  }

  numData = OPS_GetNumRemainingInputArgs();

  if (numData != 7) {
    opserr << "Invalid #args, want: uniaxialMaterial
Concrete02ThermalSCC " << iData[0] << "fpc? epsc0? fpcu? epscu? rat?
ft? Ets?\n";
    return 0;
  }

  if (OPS_GetDoubleInput(&numData, dData) != 0) {
```

```
    opserr << "Invalid #args, want: uniaxialMaterial
Concrete02ThermalSCC " << iData[0] << "fpc? epsc0? fpcu? epscu? rat?
ft? Ets?\n";
    return 0;
  }



  // Parsing was successful, allocate the material
  theMaterial = new Concrete02ThermalSCC(iData[0], dData[0], dData[1],
dData[2], dData[3], dData[4], dData[5], dData[6]);


  if (theMaterial == 0) {
    opserr << "WARNING could not create uniaxialMaterial of type
Concrete02ThermalSCC Material\n";
    return 0;
  }


  return theMaterial;
}



Concrete02ThermalSCC::Concrete02ThermalSCC(int tag, double _fc, double
_epsc0, double _fcu,
                           double _epscu, double _rat, double _ft,
double _Ets):
  UniaxialMaterial(tag, MAT_TAG_Concrete02ThermalSCC),
  //fc(_fc), epsc0(_epsc0), fcu(_fcu), epscu(_epscu), rat(_rat),
ft(_ft), Ets(_Ets)
  fcT(_fc), epsc0T(_epsc0), fcuT(_fcu), epscuT(_epscu), rat(_rat),
ftT(_ft), EtsT(_Ets) //JZ
{


//JZ 07/10
////////////////////////////////////////////////////////////start
  fc = fcT;
  epsc0 = epsc0T;
  fcu = fcuT;
  epscu = epscuT;
  ft = ftT;
  Ets = EtsT;
//JZ 07/10
////////////////////////////////////////////////////////////end
```

```
  ecminP = 0.0;
  deptP = 0.0;

  eP = 2.0*fc/epsc0;
  //eP = 1.5*fc/epsc0; //for the euro code, the 2.0 should be changed
into 1.5
  epsP = 0.0;
  sigP = 0.0;
  eps = 0.0;
  sig = 0.0;
  e = 2.0*fc/epsc0;
  //e = 1.5*fc/epsc0;//for the euro code, the 2.0 should be changed
into 1.5

  //if epsc0 is not 0.0025, then epsc0 = strainRatio*0.0025
  strainRatio = epsc0/0.0025;
  ThermalElongation = 0; //initialize

  cooling=0; //PK add
  TempP = 0.0; //Pk add previous temp

}

Concrete02ThermalSCC::Concrete02ThermalSCC(void):
  UniaxialMaterial(0, MAT_TAG_Concrete02ThermalSCC)
{

}

Concrete02ThermalSCC::~Concrete02ThermalSCC(void)
{
  // Does nothing
}




UniaxialMaterial*
Concrete02ThermalSCC::getCopy(void)
```

```
{
  Concrete02ThermalSCC *theCopy = new Concrete02ThermalSCC(this->getTag(), fc, epsc0, fcu, epscu, rat, ft, Ets);

  return theCopy;
}

double
Concrete02ThermalSCC::getInitialTangent(void)
{
  return 2.0*fc/epsc0;
}

int
Concrete02ThermalSCC::setTrialStrain(double trialStrain, double FiberTemperature, double strainRate)
{
  double    ec0 = fc * 2. / epsc0;//?
  // double       ec0 = fc * 1.5 / epsc0; //JZ. 27/07/10 ??

  // retrieve concrete hitory variables

  ecmin = ecminP;
  dept = deptP;

  // calculate current strain

  eps = trialStrain;
  double deps = eps - epsP;

  // if the current strain is less than the smallest previous strain
  // call the monotonic envelope in compression and reset minimum strain

  if (eps < ecmin) {
    this->Compr_Envlp(eps, sig, e);
    ecmin = eps;
  } else {;
```

```
    // else, if the current strain is between the minimum strain and
ept
    // (which corresponds to zero stress) the material is in the
unloading-
    // reloading branch and the stress remains between sigmin and
sigmax


    // calculate strain-stress coordinates of point R that determines
    // the reloading slope according to Fig.2.11 in EERC Report
    // (corresponding equations are 2.31 and 2.32
    // the strain of point R is epsR and the stress is sigmR

    double epsr = (fcu - rat * ec0 * epscu) / (ec0 * (1.0 - rat));
    double sigmr = ec0 * epsr;

    // calculate the previous minimum stress sigmm from the minimum
    // previous strain ecmin and the monotonic envelope in compression

    double sigmm;
    double dumy;
    this->Compr_Envlp(ecmin, sigmm, dumy);

    // calculate current reloading slope Er (Eq. 2.35 in EERC Report)
    // calculate the intersection of the current reloading slope Er
    // with the zero stress axis (variable ept) (Eq. 2.36 in EERC
Report)

    double er = (sigmm - sigmr) / (ecmin - epsr);
    double ept = ecmin - sigmm / er;

    if (eps <= ept) {
      double sigmin = sigmm + er * (eps - ecmin);
      double sigmax = er * .5f * (eps - ept);
      sig = sigP + ec0 * deps;
      e = ec0;
      if (sig <= sigmin) {
      sig = sigmin;
      e = er;
      }
      if (sig >= sigmax) {
```

```
      sig = sigmax;
      e = 0.5 * er;
      }
    } else {

      // else, if the current strain is between ept and epn
      // (which corresponds to maximum remaining tensile strength)
      // the response corresponds to the reloading branch in tension
      // Since it is not saved, calculate the maximum remaining tensile
      // strength sicn (Eq. 2.43 in EERC Report)

      // calculate first the strain at the peak of the tensile stress-
strain
      // relation epn (Eq. 2.42 in EERC Report)

      double epn = ept + dept;
      double sicn;
      if (eps <= epn) {
      this->Tens_Envlp(dept, sicn, e);
      if (dept != 0.0) {
        e = sicn / dept;
      } else {
        e = ec0;
      }
      sig = e * (eps - ept);
      } else {

      // else, if the current strain is larger than epn the response
      // corresponds to the tensile envelope curve shifted by ept

      double epstmp = eps - ept;
      this->Tens_Envlp(epstmp, sig, e);
      dept = eps - ept;
      }
    }
  }

  return 0;
}
```

```
double
Concrete02ThermalSCC::getStrain(void)
{
  return eps;
}

double
Concrete02ThermalSCC::getStress(void)
{
  return sig;
}

double
Concrete02ThermalSCC::getTangent(void)
{
  return e;
}

double
Concrete02ThermalSCC::getThermalElongation(void) //***JZ
{
  return ThermalElongation;
}

double
Concrete02ThermalSCC::getElongTangent(double TempT, double& ET, double&
Elong, double TempTmax) //PK add to include max temp
{
  //material properties with temperature
  Temp = TempT;  //make up the 20 degree which is minus in the class of
thermalfield
  Tempmax = TempTmax; //PK add max temp for cooling
  // The datas are from EN 1992 part 1-2-1
  // Tensile strength at elevated temperature

   //if (Temp >= 1080) {
  //    opserr << "temperature " << " " << Temp <<endln;
```

```
  //}
  if (Temp <= 100) {
        ft = ftT;
  }
  else if (Temp <= 800) {
        ft = (0.99 - (0.001*Temp))*ftT;
        Ets = (1.0 - 1.0*(Temp -80)/500)*fcT * 1.5 / epsc0T;
        //Ets = (1.0 - 1.0*(Temp -80)/500)*EtsT;
  }
  else {
        ft = 1.0e-3;
        Ets = 1.0e-3;
        //ft = 0;
        //Ets = 0;
  }

  // compression strength, at elevated temperature
  //   strain at compression strength, at elevated temperature
  //   ultimate (crushing) strain, at elevated temperature
  if (Temp <= 0) {
        fc = fcT;
        epsc0 = -0.0025;
        fcu = fcuT;
        epscu = -0.02;
        //Ets = EtsT;  jz what is there the statement?
  }
  else if (Temp <= 100) {
        fc = fcT;
        epsc0 = -(0.0025 + (0.004-0.0025)*(Temp - 0)/(80 - 0));
        fcu = fcuT;
        epscu = -(0.0200 + (0.0225-0.0200)*(Temp - 0)/(80 - 0));
  }
  else if (Temp <= 200) {
      fc = fcT*(0.99 - (0.002*Temp));
        epsc0 = -(0.0040 + (0.0055-0.0040)*(Temp - 80)/100);
      fcu = fcuT*(1 - (Temp - 80)*0.05/100);
        epscu = -(0.0225 + (0.0225-0.0200)*(Temp - 80)/100);
  }
//  //else if (Temp <= 280) {
```

```
//    //  fc = fcT*(0.95 - (Temp - 180)*0.1/100);
//      //epsc0 = -(0.0055 + (0.0070-0.0055)*(Temp - 180)/100);
//      fcu = fcuT*(0.95 - (Temp - 180)*0.1/100);
//      epscu = -(0.0250 + 0.0025*(Temp - 180)/100);
//  }
//  //else if (Temp <= 380) {
//       fc = fcT*(0.85 - (Temp - 280)*0.1/100);
//      epsc0 = -(0.0070 + (0.0100-0.0070)*(Temp - 280)/100);
//      fcu = fcuT*(0.85 - (Temp - 280)*0.1/100);
//      epscu = -(0.0275 + 0.0025*(Temp - 280)/100);
//  }
//  else if (Temp <= 480) {
//       fc = fcT*(0.75 - (Temp - 380)*0.15/100);
//      epsc0 = -(0.0100 + (0.0150-0.0100)*(Temp - 380)/100);
//      fcu = fcuT*(0.75 - (Temp - 380)*0.15/100);
//      epscu = -(0.03 + 0.0025*(Temp - 380)/100);
//  }
//  else if (Temp <= 580) {
//       fc = fcT*(0.60 - (Temp - 480)*0.15/100);
//      epsc0 = -(0.0150 + (0.0250-0.0150)*(Temp - 480)/100);
//      fcu = fcuT*(0.60 - (Temp - 480)*0.15/100);
//      epscu = -(0.0325 + 0.0025*(Temp - 480)/100);
//  }
//  else if (Temp <= 680) {
//       fc = fcT*(0.45 - (Temp - 580)*0.15/100);
//      epsc0 = -0.0250;
//      fcu = fcuT*(0.45 - (Temp - 580)*0.15/100);
//      epscu = -(0.035 + 0.0025*(Temp - 580)/100);
//  }
//  else if (Temp <= 780) {
//       fc = fcT*(0.30 - (Temp - 680)*0.15/100);
//      epsc0 = -0.0250;
//      fcu = fcuT*(0.30 - (Temp - 680)*0.15/100);
//      epscu = -(0.0375 + 0.0025*(Temp - 680)/100);
//  }
  else if (Temp <= 800) {
      fc = fcT*(0.73 - (0.0005*Temp));
       epsc0 = -0.0250;
       fcu = fcuT*(0.15 - (Temp - 780)*0.07/100);
```

```
        epscu = -(0.04 + 0.0025*(Temp - 780)/100);
  }
//  else if (Temp <= 980) {
//       fc = fcT*(0.08 - (Temp - 880)*0.04/100);
//       epsc0 = -0.0250;
//       fcu = fcuT*(0.08 - (Temp - 880)*0.04/100);
//       epscu = -(0.0425 + 0.0025*(Temp - 880)/100);
//  }
//  else if (Temp <= 1080) {
//       fc = fcT*(0.04 - (Temp - 980)*0.03/100);
//       epsc0 = -0.0250;
//       fcu = fcuT*(0.04 - (Temp - 980)*0.03/100);
//       epscu = -(0.045 + 0.0025*(Temp - 980)/100);
//  }
  else  {
      opserr << "the temperature is invalid\n";
  }
//jz assign a miner to the valuables

       // epsc0 = epsc0T*strainRatio;
       // epscu = epscuT*strainRatio;

  // caculation of thermal elongation
        if (Temp <= 1) {
              ThermalElongation = (Temp - 0) * 9.213e-6;
        }
  else if (Temp <= 680) {
      ThermalElongation = -1.8e-4 + 9e-6 *(Temp+20) + 2.3e-11
*(Temp+20)*(Temp+20)*(Temp+20);
  }
  else if (Temp <= 1180) {
      ThermalElongation = 14.009e-3;  //Modified by Liming,2013
  }
  else {
        opserr << "the temperature is invalid\n";
  }

  ET = 1.5*fc/epsc0;
  Elong = ThermalElongation;
```

```
  //For cooling to exist T must go to Tmax and then decrease
//if cooling the factor becomes 1
 //if (Temp = Tempmax) {
    //cooling=1;
 // }

///PK COOLING PART FOR DESCENDING BRANCH OF A FIRE////
  // If temperature is less that previous commited temp then we have
cooling taking place
  if (Temp < TempP) {

//opserr << "cooling " << Temp << " " << TempP << endln;

  double kappa;
  double fcmax; //compr strength at max temp
  double fcumax; //ultimate compr strength at max temp
  double fcamb; //compr strength at cooled ambient temp
  double fcuamb; //ultimate compr strength at cooled ambient temp
  double epsc0max; //strain at compression strength for the max temp
  double epscumax; //ultimate strain at ultimate compression strength
for the max temp
  if (TempP == Tempmax) {
    //opserr << "cooling,T,TP,Tmax " << Temp << " " << TempP << " " <<
Tempmax <<endln;
  }
  // PK Determine residual compressive strength of concrete heated to
the max temp and then having cooled down to ambient
  // This will be the same for all the timesteps during the cooling
phase
  // PK 1st step is to determine Kc,Tempmax according to table in 3.2.2
(EN1994-1-2:2005)

  if (Tempmax < 0) {
    opserr << "max temperature cannot be less than zero " << " " <<
Tempmax <<endln;
  }
  else if (Tempmax <= 80) {
    kappa = 1;
    fcmax = fcT;
    fcumax = fcuT;
```

```
}
else if (Tempmax <= 180) {
  kappa = 1 - (Tempmax - 80)*0.05/100;
  fcmax = fcT*(1 - (Tempmax - 80)*0.05/100);
  fcumax = fcuT*(1 - (Tempmax - 80)*0.05/100);
}
else if (Tempmax <= 280) {
  kappa = 0.95 - (Tempmax - 180)*0.1/100;
  fcmax = fcT*(0.95 - (Tempmax - 180)*0.1/100);
  fcumax = fcuT*(0.95 - (Tempmax - 180)*0.1/100);
}
else if (Tempmax <= 380) {
  kappa = 0.85 - (Tempmax - 280)*0.1/100;
  fcmax = fcT*(0.85 - (Tempmax - 280)*0.1/100);
  fcumax = fcuT*(0.85 - (Tempmax - 280)*0.1/100);
}
else if (Tempmax <= 480) {
  kappa = 0.75 - (Tempmax - 380)*0.15/100;
  fcmax = fcT*(0.75 - (Tempmax - 380)*0.15/100);
  fcumax = fcuT*(0.75 - (Tempmax - 380)*0.15/100);
}
else if (Tempmax <= 580) {
  kappa = 0.60 - (Tempmax - 480)*0.15/100;
  fcmax = fcT*(0.60 - (Tempmax - 480)*0.15/100);
  fcumax = fcuT*(0.60 - (Tempmax - 480)*0.15/100);
}
else if (Tempmax <= 680) {
  kappa = 0.45 - (Tempmax - 580)*0.15/100;
  fcmax = fcT*(0.45 - (Tempmax - 580)*0.15/100);
  fcumax = fcuT*(0.45 - (Tempmax - 580)*0.15/100);
}
else if (Tempmax <= 780) {
  kappa = 0.30 - (Tempmax - 680)*0.15/100;
  fcmax = fcT*(0.30 - (Tempmax - 680)*0.15/100);
  fcumax = fcuT*(0.30 - (Tempmax - 680)*0.15/100);
}
else if (Tempmax <= 880) {
  kappa = 0.15 - (Tempmax - 780)*0.07/100;
  fcmax = fcT*(0.15 - (Tempmax - 780)*0.07/100);
```

```
    fcumax = fcuT*(0.15 - (Tempmax - 780)*0.07/100);
  }
  else if (Tempmax <= 980) {
    kappa = 0.08 - (Tempmax - 880)*0.04/100;
    fcmax = fcT*(0.08 - (Tempmax - 880)*0.04/100);
    fcumax = fcuT*(0.08 - (Tempmax - 880)*0.04/100);
  }
  else if (Tempmax <= 1080) {
    kappa = 0.04 - (Tempmax - 980)*0.03/100;
    fcmax = fcT*(0.04 - (Tempmax - 980)*0.03/100);
    fcumax = fcuT*(0.04 - (Tempmax - 980)*0.03/100);
  }
  else  {
    opserr << "the temperature is invalid\n";
  }
  // PK 2nd step is to determine compressice strength at ambient after
cooling as shown in ANNEX C (EN1994-1-2:2005)
  if (Tempmax < 0) {
    opserr << "max temperature cannot be less than zero " << " " <<
Tempmax <<endln;
  }
  else if (Tempmax <= 80) {
    fcamb = kappa*fcT;
    fcuamb = kappa*fcuT;
  }
  else if (Tempmax <= 280) {
    fcamb=(1-(0.235*(Tempmax-80)/200))* fcT;
    fcuamb=(1-(0.235*(Tempmax-80)/200))* fcuT;
  }
  else if (Tempmax <= 1080) {
    fcamb = 0.9*kappa*fcT;
    fcuamb = 0.9*kappa*fcuT;
  }
  else {
    opserr << "the temperature is invalid\n";
  }

  // Calculation of current compressive strength
  // linear interpolation between ambient and maximum compressive
strength (after and before cooling)
```

```
  fc = fcmax - ((fcmax-fcamb)*(Tempmax-Temp)/Tempmax);
  fcu = fcumax - ((fcumax-fcuamb)*(Tempmax-Temp)/Tempmax);


  // Calculation of epsc0 for Tempmax and then keep it the same for all
next time steps
  if (Tempmax < 0) {
    opserr << "max temperature cannot be less than zero " << " " <<
Tempmax <<endln;
  }
  else if (Tempmax <= 80) {
    epsc0max = -(0.0025 + (0.004-0.0025)*(Tempmax - 0)/(80 - 0));
    epscumax = -(0.0200 + (0.0225-0.0200)*(Tempmax - 0)/(80 - 0));
  }
  else if (Tempmax <= 180) {
    epsc0max = -(0.0040 + (0.0055-0.0040)*(Tempmax - 80)/100);
    epscumax = -(0.0225 + (0.0225-0.0200)*(Tempmax - 80)/100);
  }
  else if (Tempmax <= 280) {
    epsc0max = -(0.0055 + (0.0070-0.0055)*(Tempmax - 180)/100);
    epscumax = -(0.0250 + 0.0025*(Tempmax - 180)/100);
  }
  else if (Tempmax <= 380) {
    epsc0max = -(0.0070 + (0.0100-0.0070)*(Tempmax - 280)/100);
    epscumax = -(0.0275 + 0.0025*(Tempmax - 280)/100);
  }
  else if (Tempmax <= 480) {
    epsc0max = -(0.0100 + (0.0150-0.0100)*(Tempmax - 380)/100);
    epscumax = -(0.03 + 0.0025*(Tempmax - 380)/100);
  }
  else if (Tempmax <= 580) {
    epsc0max = -(0.0150 + (0.0250-0.0150)*(Tempmax - 480)/100);
    epscumax = -(0.0325 + 0.0025*(Tempmax - 480)/100);
  }
  else if (Tempmax <= 680) {
    epsc0max = -0.0250;
    epscumax = -(0.035 + 0.0025*(Tempmax - 580)/100);
  }
  else if (Tempmax <= 780) {
    epsc0max = -0.0250;
```

```
    epscumax = -(0.0375 + 0.0025*(Tempmax - 680)/100);
  }
  else if (Tempmax <= 880) {
    epsc0max = -0.0250;
    epscumax = -(0.04 + 0.0025*(Tempmax - 780)/100);
  }
  else if (Tempmax <= 980) {
    epsc0max = -0.0250;
    epscumax = -(0.0425 + 0.0025*(Tempmax - 880)/100);
  }
  else if (Tempmax <= 1080) {
    epsc0max = -0.0250;
    epscumax = -(0.045 + 0.0025*(Tempmax - 980)/100);
  }
  else  {
    opserr << "the temperature is invalid\n";
  }

  //make eps0 = eps0max

  epsc0 = epsc0max;

  // Calculating epscu
  epscu = epsc0 + ((epscumax-epsc0max)*fc/fcmax);

  ft=0;

  // Make thermal elongation zero during the cooling phase
 // Elong =0;


      }
   if (Temp > 0) {
    //cooling=1;
      //opserr << "Heating,T,TP,Tmax " << Temp << " " << TempP << " "
<< Tempmax <<endln;
      }

  return 0;
}
```

```
int
Concrete02ThermalSCC::commitState(void)
{
  ecminP = ecmin;
  deptP = dept;

  eP = e;
  sigP = sig;
  epsP = eps;

  TempP = Temp; //PK add set the previous temperature

  return 0;
}

int
Concrete02ThermalSCC::revertToLastCommit(void)
{
  ecmin = ecminP;;
  dept = deptP;

  e = eP;
  sig = sigP;
  eps = epsP;

  //Temp = TempP; //PK add set the previous temperature

  // NA ELENXW MIPWS EDW XANETAI TO TEMP LOGW MIN CONVERGENCE

  return 0;
}

int
Concrete02ThermalSCC::revertToStart(void)
{
  ecminP = 0.0;
  deptP = 0.0;
```

```
  eP = 2.0*fc/epsc0;
  epsP = 0.0;
  sigP = 0.0;
  eps = 0.0;
  sig = 0.0;
  e = 2.0*fc/epsc0;

  return 0;
}

int
Concrete02ThermalSCC::sendSelf(int commitTag, Channel &theChannel)
{
  static Vector data(13);
  data(0) =fc;
  data(1) =epsc0;
  data(2) =fcu;
  data(3) =epscu;
  data(4) =rat;
  data(5) =ft;
  data(6) =Ets;
  data(7) =ecminP;
  data(8) =deptP;
  data(9) =epsP;
  data(10) =sigP;
  data(11) =eP;
  data(12) = this->getTag();

  if (theChannel.sendVector(this->getDbTag(), commitTag, data) < 0) {
    opserr << "Concrete02ThermalSCC::sendSelf() - failed to
sendSelf\n";
    return -1;
  }
  return 0;
}

int
Concrete02ThermalSCC::recvSelf(int commitTag, Channel &theChannel,
          FEM_ObjectBroker &theBroker)
```

```
{

  static Vector data(13);

  if (theChannel.recvVector(this->getDbTag(), commitTag, data) < 0) {
    opserr << "Concrete02ThermalSCC::recvSelf() - failed to
recvSelf\n";
    return -1;
  }

  fc = data(0);
  epsc0 = data(1);
  fcu = data(2);
  epscu = data(3);
  rat = data(4);
  ft = data(5);
  Ets = data(6);
  ecminP = data(7);
  deptP = data(8);
  epsP = data(9);
  sigP = data(10);
  eP = data(11);
  this->setTag(data(12));

  e = eP;
  sig = sigP;
  eps = epsP;

  return 0;
}

void
Concrete02ThermalSCC::Print(OPS_Stream &s, int flag)
{
  s << "Concrete02ThermalSCC:(strain, stress, tangent) " << eps << " "
<< sig << " " << e << endln;
}



void
```

```
Concrete02ThermalSCC::Tens_Envlp (double epsc, double &sigc, double
&Ect)
{
/*-----------------------------------------------------------------------
--
! monotonic envelope of concrete in tension (positive envelope)
!
!   ft    = concrete tensile strength
!   Ec0   = initial tangent modulus of concrete
!   Ets   = tension softening modulus
!   eps   = strain
!
!   returned variables
!    sigc  = stress corresponding to eps
!    Ect  = tangent concrete modulus
!-----------------------------------------------------------------------
-*/

  double Ec0  = 2.0*fc/epsc0;
      // double Ec0  = 1.5*fc/epsc0;

  double eps0 = ft/Ec0;
  double epsu = ft*(1.0/Ets+1.0/Ec0);
  if (epsc<=eps0) {
    sigc = epsc*Ec0;
    Ect  = Ec0;
  } else {
    if (epsc<=epsu) {
      Ect  = -Ets;
      sigc = ft-Ets*(epsc-eps0);
    } else {
      //      Ect  = 0.0
      Ect  = 1.0e-10;
      sigc = 0.0;
    }
  }
  return;
}
```

```
void
Concrete02ThermalSCC::Compr_Envlp (double epsc, double &sigc, double
&Ect)
{
/*-----------------------------------------------------------------
--
! monotonic envelope of concrete in compression (negative envelope)
!
!   fc    = concrete compressive strength
!   epsc0 = strain at concrete compressive strength
!   fcu   = stress at ultimate (crushing) strain
!   epscu = ultimate (crushing) strain
!   Ec0   = initial concrete tangent modulus
!   epsc  = strain
!
!   returned variables
!   sigc  = current stress
!   Ect   = tangent concrete modulus
-----------------------------------------------------------------
*/

  double Ec0  = 2.0*fc/epsc0;
  //double Ec0  = 1.5*fc/epsc0;

  double ratLocal = epsc/epsc0;
  if (epsc>=epsc0) {
    sigc = fc*ratLocal*(2.0-ratLocal);
    Ect  = Ec0*(1.0-ratLocal);
  } else {

    //   linear descending branch between epsc0 and epscu
    if (epsc>epscu) {
      sigc = (fcu-fc)*(epsc-epsc0)/(epscu-epsc0)+fc;
      Ect  = (fcu-fc)/(epscu-epsc0);
    } else {

      // flat friction branch for strains larger than epscu

      sigc = fcu;
      Ect  = 1.0e-10;
```

```
      //       Ect  = 0.0
    }
  }
  return;
}

int
Concrete02ThermalSCC::getVariable(const char *varName, Information
&theInfo)
{
  if (strcmp(varName,"ec") == 0) {
    theInfo.theDouble = epsc0;
    return 0;
  } else if (strcmp(varName,"ElongTangent") == 0) {
    Vector *theVector = theInfo.theVector;
    if (theVector != 0) {
      double tempT, ET, Elong, TempTmax;
      tempT = (*theVector)(0);
        ET = (*theVector)(1);
        Elong = (*theVector)(2);
      TempTmax = (*theVector)(3);
      this->getElongTangent(tempT, ET, Elong, TempTmax);
        (*theVector)(0) = tempT;
      (*theVector)(1) = ET;
      (*theVector)(2) = Elong;
        (*theVector)(3) = TempTmax;
    }
    return 0;
  }
  return -1;
}



//this function is no use, just for the definiation of pure virtual
function.
int
Concrete02ThermalSCC::setTrialStrain(double strain, double strainRate)
{
```

```
  opserr << "Concrete02ThermalSCC::setTrialStrain(double strain, double
strainRate) - should never be called\n";
  return -1;
}
```

APPENDIX D

EXAMPLE CODE GIVEN IN OFFICIAL SITE OF OPENSEES FOR DEVELPERS

```
##############################################################################
#########
# composite beam with single section.
# total 10 elements for 10000mm beam ;
# distributed load UDL=10N/mm; thermal gradient is linear cross section;
# 8 fibers for both the slab and steel beam section;
# Material class Steel01Thermal is used for steel and Concrete02Thermal for concrete;
# unit i.e. mm, KN, MPa
# Written: Jian Jiang
# August 2012, University of Edinburgh
#
# sketch of composite beam (9m)-------------------------------------------------------
#       ^Y
#       |
#      \|                                              |/
#      \|-----------------------------------------------------------------|/----->X
#      \| 1   2     3     4     5     6     7     8     9     10    11|/
#
```

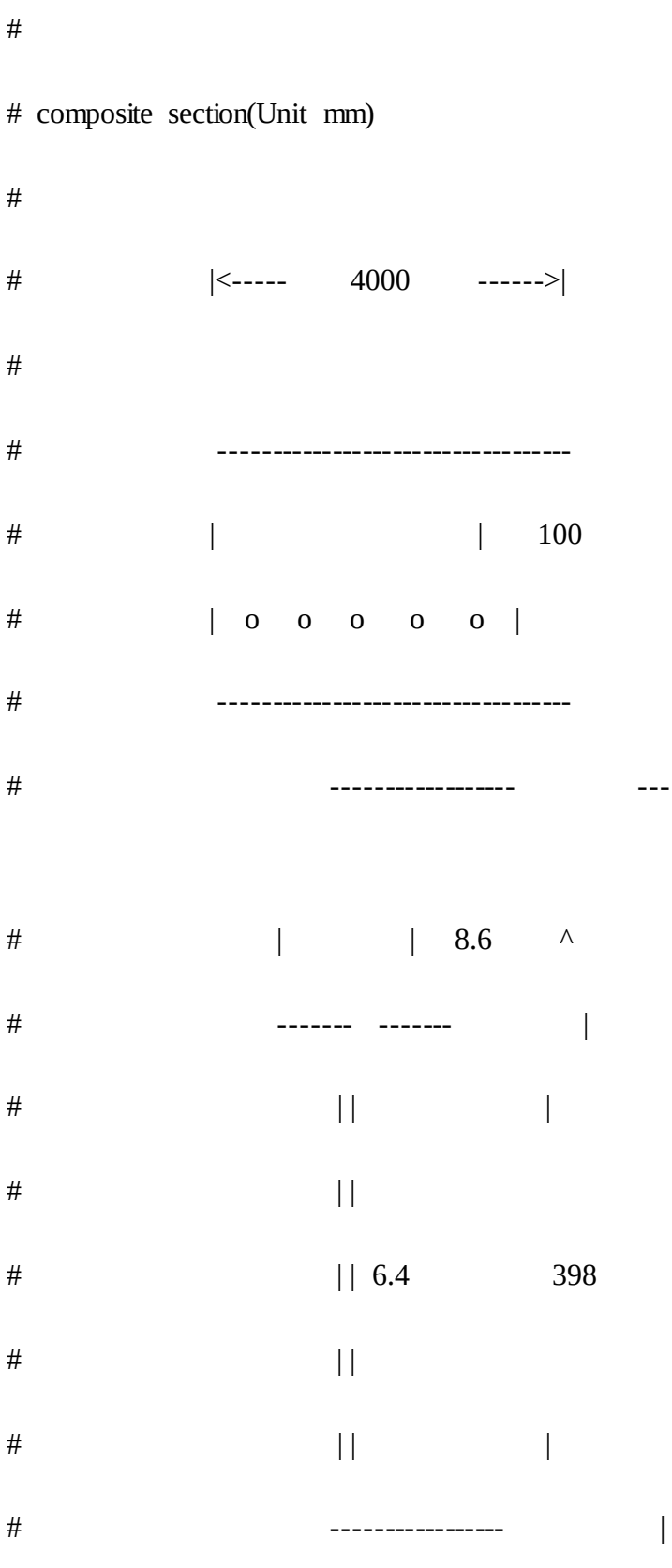
composite section(Unit mm)
|<----- 4000 ------>|
100
8.6
6.4
398
8.6

```
#                       ----------------          ---
#
#                       |<---  141.8 --->|
# SET UP ---------------------------------------------------------------------------

wipe;
model BasicBuilder  -ndm 2 -ndf 3;

source DisplayPlane.tcl
source DisplayModel2D.tcl

# define  NODAL COORDINATES  FOR composite  beam
for {set level  1} {$level  <=11} {incr  level  1} {
        set X [expr ($level-1)*1000];
        set nodeID $level
        node $nodeID $X 0;          # actually  define  node
}

fix  1 1 1 1;
fix  11 1 1 1;
```

```
uniaxialMaterial  Steel01Thermal  1 300 2e5 0.01;

uniaxialMaterial  Steel01Thermal  3 475 2.1e5 0.01;


set fpc -30

set epsc0 -0.003

set fpcu [expr $fpc*0.05];

set epsU -0.02

set lambda  0.1

set ft 0.0

set Ets [expr $ft/0.002];


uniaxialMaterial  Concrete02Thermal  2 $fpc $epsc0 $fpcu $epsU $lambda  $ft $Ets


#Concrete section

section fiberSecThermal  2   {

   #slab section

         fiber  -43.75 0 50000 2;

         fiber  -31.25 0 50000 2;

         fiber  -18.75 0 50000 2;

         fiber  -6.25 0 50000 2;

         fiber  6.25 0 50000 2;
```

```
        fiber  18.75 0 50000 2;

        fiber  31.25 0 50000 2;

        fiber  43.75 0 50000 2;

        layer  straight  3 13 28.275 -25 -1950 -25 1950


        #I steel  beam section

#fiber  -52.15 0 609.74 1;

#fiber  -56.45 0 609.74 1;

#fiber  -82.4 0 304.64 1;

#fiber  -130 0 304.64 1;

#fiber  -177.6 0 304.64 1;

#fiber  -225.2 0 304.64 1;

#fiber  -272.8 0 304.64 1;

#fiber  -320.4 0 304.64 1;

#fiber  -368 0 304.64 1;

#fiber  -415.6 0 304.64 1;

#fiber  -441.55 0 609.74 1;

#fiber  -445.85 0 609.74 1;


        }
```

```
geomTransf Corotational 1;


#ELES FOR composite BEAMS
for {set level 1} {$level <=10} {incr level 1} {
        set node1 $level
        set node2 [expr $node1+1]
        set eleID $level
        element dispBeamColumnThermal $eleID $node1 $node2 5 2 1;          # actually
define element
}


recorder Node -file node6_SingleSection.out -time -node 6 -dof 2 disp;


# apply UDL
pattern Plain 1 Linear {
#CREATE UNIFORM LOADS FOR BEAMS
set UDL -0;
for {set level 1} {$level <= 10} {incr level 1} {
        set eleID $level
        eleLoad -ele $eleID -type -beamUniform $UDL 0
```

```
}

}


constraints Plain;

numberer Plain;

system BandGeneral;

test NormUnbalance 1.0e-2 12;

algorithm Newton;

integrator LoadControl 1;

analysis Static;

analyze 1;


loadConst -time 0.0


# Define DISPLAY ----------------------------------------------------------

set xPixels 1000;       # height of graphical window in pixels

set yPixels 490;        # height of graphical window in pixels

set xLoc1 10; # horizontal location of graphical window (0=upper left-most corner)

set yLoc1 10; # vertical location of graphical window (0=upper left-most corner)

set ViewScale 0.0000002;     # scaling factor for viewing deformed shape, it depends on the dimensions of the model
```

```
DisplayModel2D DeformedShape $ViewScale $xLoc1 $yLoc1 $xPixels $yPixels 0


#define thermal load
# apply thermal load, temperature is linearly distributed through section
# bottom and top temp of steel beam is 1000 and 600;
# bottom and top temp of slab is 600 and 0;
set T1 800;set T2 600; set T3 450; set T4 300; set T5 0;
set Y1 -448; set Y2 -50;set Y3 -25;set Y4 0;set Y5 50;
pattern Plain 2 Linear {
for {set level 1} {$level <=10} {incr level 1} {
set eleID $level
eleLoad -ele $eleID -type -beamThermal $T1 $Y1 $T2 $Y3 $T3 $Y3 $T4 $Y4 $T5 $Y5;
}
}
test NormUnbalance 1.0e-2 100;
algorithm Newton;
integrator LoadControl 0.01;
analysis Static;
analyze 100;
```

APPENDIX E

E.1 Design of beams

This appendix summarizes the design calculations using ACI 318 (2008) provisions for an NSC beam and an HSC beam. The cross-section, shear force diagram, and bending moment diagram for the tested beams are shown in Figure B.1. The design calculations are presented in the following two sections.

E.1.1 Normal strength concrete beam

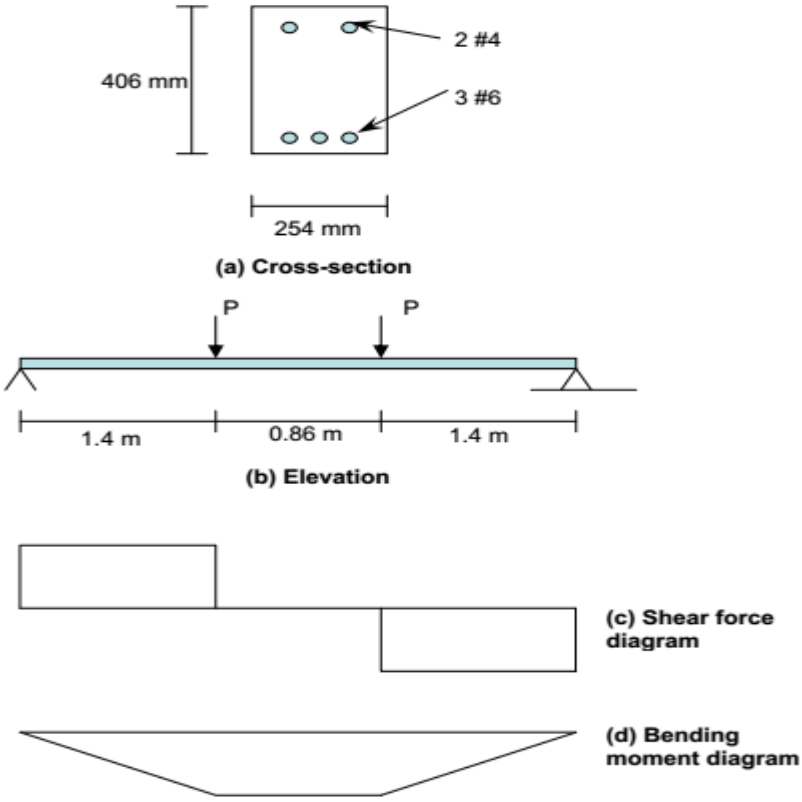

Figure E-12.1 Cross-section, Elevation, Shear Force Diagram, and Bending Moment

$f'_c = 41.3\,\text{MPa}$ $f_y = 413\,\text{MPa}$

Neglecting the area of steel in the compression zone:

The tensile area of steel $A_s = 855\ \text{mm}^2$

Clear concrete cover = 38 mm

$h = 406$ mm $b = 254$ mm

$d = 352.4$ mm

$a = 39.6\,\text{mm}$

$a = \beta_1\, c$

Hence, $\beta_1 = 0.75$

Therefore, $c = \dfrac{39.6}{0.75} = 52.8\,\text{mm}$

Strain in tensile steel can be calculated by interpolation as follows:

$$\varepsilon_t = \frac{0.003}{c}(d-c) = \frac{0.003}{52.8}(352.4-52.8) = 0.017 > 0.005$$

Hence, $\phi = 0.9$

Check minimum reinforcement:

$\rho_{min} = 0.0039$

$$\rho = \frac{A_s}{bd} = 0.00955 > \rho_{min}$$

The moment capacity of the beam is

$$M_n = A_s f_y\left(d - \frac{a}{2}\right) = \frac{855 \times 413 \times \left(352.4 - \dfrac{39.6}{2}\right)}{10^6} = 117\,\text{kN.m}$$

$$M_n = 1.4P_n$$

$$P_n = 83.9 \text{ kN} \qquad \text{and } P_u = 75.5 \text{ kN}$$

Design for shear:

The ultimate shear force is at distance *d* from the face of the support:

$$V_u = P_u = 75.5 \text{ kN}$$

Required nominal shear strength:

$$\phi = 0.75$$

$$V_n = \frac{V_u}{\phi} = \frac{75.5}{0.75} = 100.7 \text{ kN}$$

The concrete shear strength is:

$$V_c = 0.16\sqrt{f'_c} b_w d = \frac{0.16\sqrt{41.3} * 254 * 352.4}{1000} = 92 \text{ kN}$$

The required shear strength obtained by shear reinforcement must be:

$$V_n > V_c$$

$$V_S = V_n - V_C = 100.7 - 92 = 8.7 \text{ kN}$$

$$V_{s\,min} = max\begin{Bmatrix} 0.344 b_w d \\ 0.06\sqrt{f'_c} b_w d \end{Bmatrix} = 35 \text{ kN}$$

Use minimum shear reinforcement

The required shear reinforcement will be found to be

$$\frac{A_v}{s} = 0.237 \text{ mm}$$

Using #2 stirrups

The area of each leg is 31.6 mm^2

Hence, A_v =2×31.6 = 63.2 mm^2

The required spacing will be:

$$s = \frac{63.2}{0.237} = 267 \text{ mm} \le \frac{d}{2} = \frac{352.4}{2} = 176.2 \text{ mm} \qquad \textit{(ACI 318 11.5.4.1)}$$

Hence, use #2 stirrups 150 mm c/c

Check deflection:

The gross moment of inertia (neglecting the compressive and tensile steel) can be calculated as:

$$I_g = \frac{bh^3}{12} = 1.416\times10^9 \text{ mm}^4$$

The cracked moment of inertia (neglecting the compressive steel) can be calculated as follows:

$$E_s = 210 \text{ GPa}$$

$$E_c = 4730\sqrt{f'_c} = 30.4 \text{ GPa}$$

$$n = \frac{E_s}{E_c} = 6.9$$

$$x = \frac{\sqrt{(nA_s)^2 + 2bdnA_s} - nA_s}{b} = 106.9 \text{ mm}$$

$$I_{cr} = \frac{bx^3}{3} + nA_s(d-x)^2$$

$$I_{cr} = 0.459\times10^9 \text{ mm}^4$$

The modulus of rupture is:

$$f_r = 0.6\sqrt{f'_c} = 3.86 \text{ MPa}$$

The cracking moment is

$$M_{cr} = \frac{f_r I_g}{y_t} = 26.9 \text{ kN.m}$$

The effective moment of inertia will be:

Assume M_a to be $0.7M_u$, then

$M_a = 0.7\times117\times0.9 = 73.71$ kN.m

$$I_e = \left(\frac{M_{cr}}{M_a}\right)^3 I_g + \left[1-\left(\frac{M_{cr}}{M_a}\right)^3\right] I_{cr} \le I_g$$

$I_e = 0.506 \times 10^9 \text{ mm}^4$

Hence, the deflection of the beam will be:

$$\delta = \frac{M}{2E_c I_e}\left(\frac{L^2}{4} - \frac{a^2}{3}\right) = 6.5 \text{ mm}$$

B.1.2 High Strength Concrete Beam

$f'_c = 100 \text{ MPa}$ $f_y = 413 \text{ MPa}$

Neglecting the area of steel in the compression zone:

The tensile area of steel $A_s = 855 \text{ mm}^2$

Clear concrete cover = 38 mm

$h = 406$ mm $b = 254$ mm

$d = 352.4$ mm

$a = 16.4 \text{ mm}$

$a = \beta_1 c$

Hence, $\beta_1 = 0.65$

Therefore, $c = \frac{39.6}{0.65} = 25.2 \text{ mm}$

Strain in tensile steel can be calculated by interpolation as follows:

$$\varepsilon_t = \frac{0.003}{c}(d - c) = \frac{0.003}{25.2}(352.4 - 25.2) = 0.039 > 0.005$$

Hence, $\phi = 0.9$

Check minimum reinforcement:

$\rho_{min} = 0.006$

$$\rho = \frac{A_s}{bd} = 0.00955 > \rho_{min}$$

The moment capacity of the beam is

$$M_n = A_s f_y \left(d - \frac{a}{2} \right) = \frac{855 \times 413 \times \left(352.4 - \frac{16.4}{2} \right)}{10^6} = 121.6 \text{ kN.m}$$

$$M_n = 1.4 P_n$$

$$P_n = 86.8 \text{ kN} \qquad \text{and } P_u = 78.1 \text{ kN}$$

Design for shear:

The ultimate shear force is at distance *d* from the face of the support:

$$V_u = P_u = 78.1 \text{ kN}$$

Required nominal shear strength:

$$\phi = 0.75$$

$$V_n = \frac{V_u}{\phi} = \frac{78.1}{0.75} = 104.2 \text{ kN}$$

The concrete shear strength is:

$$V_c = 0.16 \sqrt{f'_c} b_w d = \frac{0.16 \sqrt{100} * 254 * 352.4}{1000} = 165 \text{ kN}$$

The required shear strength obtained by shear reinforcement must be:

$$V_n < V_c \qquad V_n > \frac{V_c}{2}$$

Use minimum shear reinforcement

$$V_{S\,min} = max \begin{Bmatrix} 0.344 b_w d \\ 0.06 \sqrt{f'_c} b_w d \end{Bmatrix} = 53.7 \text{ kN}$$

The required shear reinforcement may be calculated by

$$\frac{A_V}{s} = 0.369 \text{ mm}$$

Using #2 stirrups

The area of each leg is 31.6 mm^2

Hence, A_v =2*31.6 = 63.2 mm^2

The required spacing will be:

$$s = \frac{63.2}{0.369} = 171 \text{ mm}$$

Hence, use # 2 stirrups 150 mm c/c

Check deflection:

The gross moment of inertia (neglecting the compressive and tensile steel) can be calculated as:

$$I_g = \frac{bh^3}{12} = 1.416 \times 10^9 \text{ mm}^4$$

The cracked moment of inertia (neglecting the compressive steel) can be calculated as follows:

$$E_S = 210 \text{ GPa}$$

$$E_C = 4730\sqrt{f_c'} = 47.3 \text{ GPa}$$

$$n = \frac{E_s}{E_c} = 4.4$$

$$x = \frac{\sqrt{(nA_s)^2 + 2bdnA_s} - nA_s}{b} = 88.8 \text{ mm}$$

$$I_{cr} = \frac{bx^3}{3} + nA_s(d-x)^2$$

$$I_{cr} = 0.323 \times 10^9 \text{ mm}^4$$

The modulus of rupture is:

$$f_r = 0.6\sqrt{f_c'} = 6 \text{ MPa}$$

The cracking moment is

$$M_{cr} = \frac{f_r I_g}{y_t} = 41.9 \text{ kN.m}$$

The effective moment of inertia will be:

Assume M_a to be $0.7M_u$, then

$M_a = 0.7 \times 121.6 \times 0.9 = 76.6$ kN.m

$$I_e = \left(\frac{M_{cr}}{M_a}\right)^3 I_g + \left[1 - \left(\frac{M_{cr}}{M_a}\right)^3\right] I_{cr} \le I_g$$

$$I_e = 0.501 \times 10^9 \text{ mm}^4$$

Hence, the deflection of the beam will be:

$$\delta = \frac{M}{2E_c I_e}\left(\frac{L^2}{4} - \frac{a^2}{3}\right) = 4.4 \text{ mm}$$

B.2 Load Calculations

This appendix summarizes the load calculations using ACI 318 (2008) provisions for an NSC beam and an HSC beam, which were tested in the experimental program. The shear force diagram and bending moment diagram for the tested beams are shown in Figure B.2. The load calculations are presented in the following two sections.

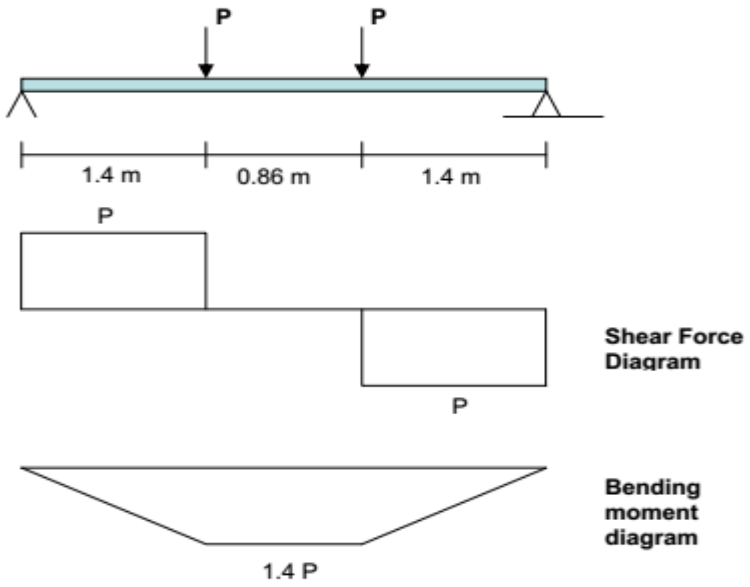

Figure E-12.2 Shear Force Diagram and Bending Moment Diagram for Tested

E.2.1 Normal strength concrete beam

$f_c' = 58.2\,\text{MPa}$ $f_y = 450\,\text{MPa}$

Neglecting the area of steel in the compression zone:

The tensile area of steel $A_s = 855\ \text{mm}^2$

Clear concrete cover = 38 mm

$h = 406$ mm $b = 254$ mm

$d = 352.4$ mm

$a = 30.6\,\text{mm}$

$a = \beta_1\, c$

Hence, $\beta_1 = 0.65$

Therefore, $c = \frac{30.6}{0.65} = 47.1\,\text{mm}$

Strain in tensile steel can be calculated by interpolation as follows:

$$\varepsilon_t = \frac{0.003}{c}(d-c) = \frac{0.003}{47.1}(352.4-47.1) = 0.019 > 0.005$$

Hence, $\phi = 0.9$

Check minimum reinforcement:

$\rho_{\min} = 0.0042$

$$\rho = \frac{A_s}{bd} = 0.00955 > \rho_{\min}$$

The moment capacity of the beam is

$$M_n = A_s f_y\left(d - \frac{a}{2}\right) = \frac{855 \times 450 \times \left(352.4 - \frac{30.6}{2}\right)}{10^6} = 129.7\,\text{kN.m}$$

The nominal load can be calculate as follows

$M_n = 1.4P_n$

$P_n = 92.7$ kN

The load ratio is defined as the ratio of applied load under fire conditions to the capacity of the section at room temperature (Buchanan 2002). Accordingly, the load ratio is given as:

$$LR = \frac{50}{92.7} \times 100\ \% = 54\%$$

E.2.2 High strength concrete beam

$f_c' = 106.5\,\text{MPa}$ $f_y = 450\,\text{MPa}$

Neglecting the area of steel in the compression zone:

The tensile area of steel $A_s = 855\ \text{mm}^2$

Clear concrete cover = 38 mm

$h = 406$ mm $\qquad b = 254$ mm

$d = 352.4$ mm

$a = 16.7$ mm

$a = \beta_1 c$

Hence, $\beta_1 = 0.65$

Therefore, $c = \dfrac{16.7}{0.65} = 25.7\,\text{mm}$

Strain in tensile steel can be calculated by interpolation as follows:

$$\varepsilon_t = \frac{0.003}{c}(d - c) = \frac{0.003}{48.7}(352.4 - 48.7) = 0.038 > 0.005$$

Hence, $\phi = 0.9$

Check minimum reinforcement:

$\rho_{\min} = 0.0057$

$$\rho = \frac{A_s}{bd} = 0.00955 > \rho_{\min}$$

The moment capacity of the beam is

$$M_n = A_s f_y\left(d - \frac{a}{2}\right) = \frac{855 \times 450 \times \left(352.4 - \dfrac{16.7}{2}\right)}{10^6} = 132.4\,\text{kN.m}$$

The nominal load can be calculate as follows

$M_n = 1.4P_n$

$P_n = 94.5$ kN

Thus, the load ratio is given as:

$$LR = \frac{50}{94.5} \times 100\ \% = 53\%$$

For 60 kN load under fire the load ratio will be:

$$LR = \frac{60}{94.5} \times 100\ \% = 63\%$$

B.3 Stress Strain Curves for Reinforcing Steel

The stress strain relationships determined via testing for the tension reinforcement used in the tested beams are shown in Figure B.3.

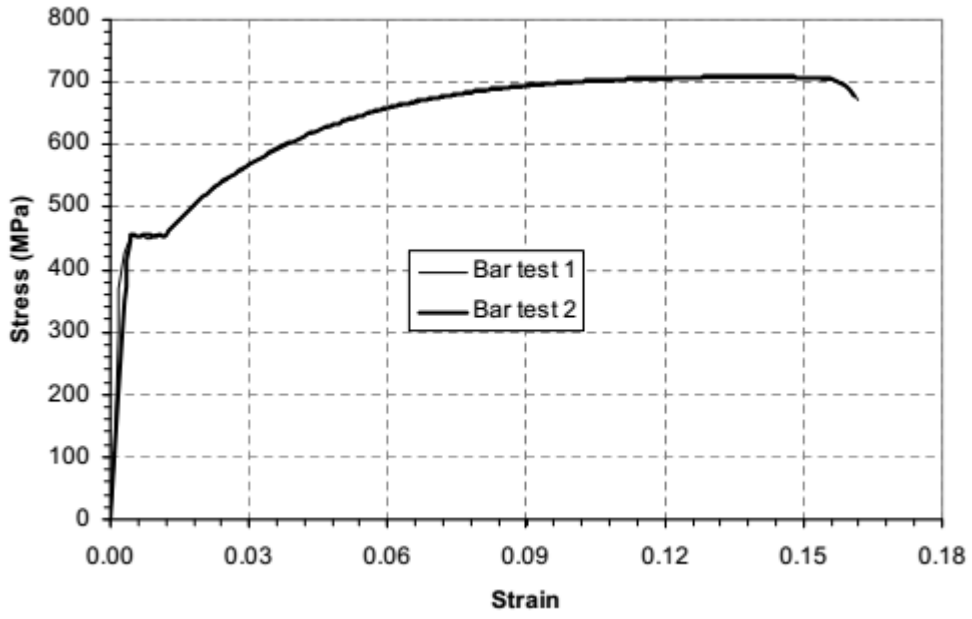

Figure 12.3 Stress Strain Curves for Steel Reinforcement used in the Tested Beams

REFERENCES

Anagnostopoulos, N., Sideris, K., and Georgiadis, A. (2009). "Mechanical characteristics of self-compacting concretes with different filler materials, exposed to elevated temperatures." *Materials and structures*, 42(10), 1393.

Bamonte, P., Gambarova, P., and Nafarieh, A. "On high-temperature properties of structural shotcrete containing different accelerating agents." *Proc., Proc. 6th Int. Conf."Structures in Fire*, 848-855.

Bazant, Z. P., and Kaplan, M. F. (1996). *Concrete at high temperatures: material properties and mathematical models*, Longman.

Behnood, A., and Ghandehari, M. (2009). "Comparison of compressive and splitting tensile strength of high-strength concrete with and without polypropylene fibers heated to high temperatures." *Fire Safety Journal*, 44(8), 1015-1022.

Buchanan, P. M. (2002). "Shrinkage of latex-modified and microsilica concrete overlay mixtures."

Castillo, C., and Durrani, A. (1990). "EFFECT OF TRANSIENT HIGH-TEMPERATURE ON HIGH-STRENGTH CONCRETE-CLOSURE." AMER CONCRETE INST 38800 INTERNATIONAL WAY, COUNTRY CLUB DRIVE, PO BOX 9094, FARMINGTON HILLS, MI 48333-9094, 653-653.

Chan, Y., Peng, G., and Anson, M. (1999). "Residual strength and pore structure of high-strength concrete and normal strength concrete after exposure to high temperatures." *Cement and Concrete Composites*, 21(1), 23-27.

Chen, B., and Liu, J. (2004). "Residual strength of hybrid-fiber-reinforced high-strength concrete after exposure to high temperatures." *Cement and Concrete Research*, 34(6), 1065-1069.

Cheng, F.-P., Kodur, V., and Wang, T.-C. (2004). "Stress-strain curves for high strength concrete at elevated temperatures." *Journal of Materials in Civil Engineering*, 16(1), 84-90.

DiNenno, P. J. (2008). *SFPE handbook of fire protection engineering*, SFPE.

Dwaikat, M. (2009). *Flexural response of reinforced concrete beams exposed to fire*, MICHIGAN STATE UNIVERSITY.

Dwaikat, M. B. (2009). *Flexural response of reinforced concrete beams exposed to fire*, Michigan State University.

Felicetti, R., Gambarova, P., Rosati, G., Corsi, F., and Giannuzzi, G. "Residual mechanical properties of high-strength concretes subjected to hightemperature cycles." *Proc., 4th Int. Symp. on Utilization of high-strenght concrete*, 579-588.

Felicetti, R., and Gambarova, P. G. (1998). "Effects of high temperature on the residual compressive strength of high-strength siliceous concretes." *ACI materials Journal*, 95, 395-406.

Furumura, F., Ave, T., Shinohara, Y., and ABE, T. "Mechanical properties of high strength concrete at high temperatures." *Proc., Proceedings of the Fourth Weimar Workshop on High Performance Concrete*, 237-252.

Harmathy, T., and Allen, L. "Thermal properties of selected masonry unit concretes." *Proc., Journal Proceedings*, 132-142.

Harmathy, T., and Research, N. R. C. C. D. o. B. (1967). *A comprehensive creep model*, Division of Building Research, National Research Council.

Jiang, J., Jiang, L., Kotsovinos, P., Zhang, J., Usmani, A., McKenna, F., and Li, G.-Q. (2013). "OpenSees software architecture for the analysis of structures in fire." *Journal of Computing in Civil Engineering*, 29(1).

Khaliq, W., and Kodur, V. (2013). "Behavior of high strength fly ash concrete columns under fire conditions." *Materials and structures*, 46(5), 857-867.

Khoury, G. A. (2000). "Effect of fire on concrete and concrete structures." *Progress in Structural Engineering and Materials*, 2(4), 429-447.

Kodur, V., and Ahmed, A. (2010). "Numerical model for tracing the response of FRP-strengthened RC beams exposed to fire." *Journal of Composites for Construction*, 14(6), 730-742.

Kodur, V., and Harmathy, T. (2008). "Properties of Building Materials, SFPE Handbook of Fire Protection Engineering, PJ DiNenno, Ed." *National Fire Protection Association, Quincy, Mass, USA*.

Kodur, V., and Sultan, M. (2003). "Effect of temperature on thermal properties of high-strength concrete." *Journal of materials in civil engineering*, 15(2), 101-107.

Kodur, V., Wang, T., and Cheng, F. (2004). "Predicting the fire resistance behaviour of high strength concrete columns." *Cement and Concrete Composites*, 26(2), 141-153.

Kodur, V. K. R. "Spalling in High Strength Concrete Exposed to Fire: Concerns, Causes, Critical Parameters and Cures." *Advanced Technology in Structural Engineering*, 1-9.

Kodur, V. K. R., and Sultan, M. A. (1998). "Structural behaviour of high strength concrete columns exposed to fire." National Research Council Canada.

Kumar, A., and Kumar, V. (2003). "Behaviour of RCC beams after exposure to elevated temperatures." *Journal of the Institution of Engineers. India. Civil Engineering Division*, 84(nov), 165-170.

Lie, T. "Structural fire protection." American Society of Civil Engineers.

Lie, T., and Kodur, V. (1996). "Thermal and mechanical properties of steel-fibre-reinforced concrete at elevated temperatures." *Canadian Journal of Civil Engineering*, 23(2), 511-517.

Lie, T. T., and Kodur, V. K. R. (1995). "Thermal properties of fibre-reinforced concrete at elevated temperatures."

Mehta, P., and Monteiro, P. (2006). "Microstructure and properties of hardened concrete." *Concrete: Microstructure, properties and materials*, 41-80.

Painter, G. C. K. (1982). "Sustained high temperature effect on concretes made with normal portland cement, normal portland cement and slag, or normal portland cement and fly ash." *Concrete International*, 4(07).

Persson, B. (2004). "Fire resistance of self-compacting concrete, SCC." *Materials and structures*, 37(9), 575-584.

Phan, L. T. (1996). *Fire performance of high-strength concrete: A report of the state-of-the art*, US Department of Commerce, Technology Administration, National Institute of Standards and Technology, Office of Applied Economics, Building and Fire Research Laboratory.

Phan, L. T., and Carino, N. J. (1998). "Review of mechanical properties of HSC at elevated temperature." *Journal of Materials in Civil Engineering*, 10(1), 58-65.

Saad, M., Abo-El-Enein, S., Hanna, G., and Kotkata, M. (1996). "Effect of temperature on physical and mechanical properties of concrete containing silica fume." *Cement and Concrete Research*, 26(5), 669-675.

Schneider, U. (1988). "Concrete at high temperatures—a general review." *Fire safety journal*, 13(1), 55-68.

Shin, K.-Y., Kim, S.-B., Kim, J.-H., Chung, M., and Jung, P.-S. (2002). "Thermo-physical properties and transient heat transfer of concrete at elevated temperatures." *Nuclear Engineering and Design*, 212(1), 233-241.

Tang, W., and Lo, T. (2009). "Mechanical and fracture properties of normal-and high-strength concretes with fly ash after exposure to high temperatures." *Magazine of Concrete Research*, 61(5), 323-330.

Usmani, A., Zhang, J., Jiang, J., Jiang, Y., and May, I. (2012). "Using OpenSees for structures in fire." *Journal of Structural Fire Engineering*, 3(1), 57-70.

Van Geem, M. G., Gajda, J., and Dombrowski, K. (1997). "Thermal properties of commercially available high-strength concretes." *Cement, Concrete and Aggregates*, 19(1), 38-54.

Williams, B., Kodur, V., Green, M. F., and Bisby, L. (2008). "Fire endurance of fiber-reinforced polymer strengthened concrete T-beams." *ACI structural Journal*, 105(1), 60.